Environmental Science and Pollution Research (2023) 30:83845–83872
https://doi.org/10.1007/s11356-023-27844-y

RESEARCH ARTICLE

Flood discharge prediction using improved ANFIS model combined with hybrid particle swarm optimisation and slime mould algorithm

Sandeep Samantaray[1] · Pratik Sahoo[2] · Abinash Sahoo[2] · Deba P. Satapathy[2]

Received: 29 January 2023 / Accepted: 19 May 2023 / Published online: 23 June 2023

Abstract

Due to the disastrous socio-economic impacts of flood hazards and estimated rise of its occurrences in the near future, there has been an increase in the importance of flood prediction worldwide. Artificial intelligence (AI) models have contributed significantly by giving cost-effective solutions for simulating physical processes of flood events and improving accuracy in prediction over the last few decades. This paper presents a novel conjoint model to forecast river flood discharge (Q_{FD}) considering data from four gauging stations of River Brahmani, Odisha India. The developed hybridised metaheuristic algorithm, i.e. ANFIS-PSOSMA, improves exploration capability of Slime mould algorithm (SMA) by integrating it with particle swarm optimisation (PSO). Performance of novel hybrid model is assessed by utilising quantitative statistical measures like the coefficient of correlation (R^2), Nash–Sutcliffe Model Efficiency (N_{SE}), root mean square error (RMSE), and mean absolute error (MAE). The proposed hybrid ANFIS model using optimisation algorithm provided the best performance values with N_{SE} of 0.9952, R^2 of 0.9946, RMSE of 0.0485, and MAE of 0.0265 during training and N_{SE} of 0.9736, R^2 of 0.9731, RMSE of 8.4236, and MAE of 4.3197 during testing at Jenapur gauging station, indicating the prospective of utilising the developed models in forecasting flood discharge. The present study's importance lies in integrating several input parameters, and AI algorithms have been utilised for developing flood prediction model. In addition, the attained results indicated that combining the optimisation algorithms with ANFIS enhanced its performance in modelling monthly flood discharge time series.

Keywords Flood discharge · Artificial intelligence · ANFIS-PSOSMA · River Brahmani

Introduction

The pressure of population growth, industrialisation, upgraded living standards, and urbanisation has led to increased water requirements and consumption (Zhou et al. 2002). Accurate and reliable flood forecasts are vital, predominantly in flood-affected regions. Unlike any other natural disaster, floods affect countless lives, property, infrastructure, and cause limitless destruction. An accurate flood forecast with proper lead time can provide forward-thoughtful attentiveness to an impending flood event early enough to minimise flood damage significantly. It is not possible to have complete protection from flooding; however, countless lives and vast amounts of money can be avoided by timely and precise predictions of the crests, magnitude, and duration of the flood. The control of floods is essential to halting climate change. In order to adjust to a changing environment and climate, flood management innovation is vital. Ineffective flood management has serious repercussions. Each year,

Responsible Editor: Marcus Schulz

✉ Sandeep Samantaray
samantaraysandeep963@gmail.com

Pratik Sahoo
sahoopratikps@gmail.com

Abinash Sahoo
bablusaoo1992@gmail.com

Deba P. Satapathy
dpsatapathy@cet.edu.in

[1] Department of Civil Engineering, NIT Srinagar, Jammu and Kashmir, India

[2] Department of Civil Engineering, OUTR Bhubaneswar, Odisha, India

flooding causes up to tens of billions of dollars worth of economic damage and hundreds of fatalities worldwide. Because of machine learning (ML) algorithm's strong authority in unravelling non-linear relationships, they have been broadly employed for solving environmental and hydrological problems (Fan et al. 2019; Xiao et al. 2019; Yaseen et al. 2019; Deo et al. 2016). Data-driven models (DDM) work on the basis of functional connections between input (e.g. independent) and target (e.g. dependent) variables (Liang et al. 2019; Kim et al. 2019). In hydrological studies, DDM, using ML algorithms, has been extensively utilised and has revealed better prediction performances with lesser constraints compared to physical-based models (Mosavi et al. 2018; Zia et al. 2015; Samantaray et al. 2022f). Classic DDM for hydrological investigations comprises artificial neural networks (ANN; McCulloch and Pitts 1943), support vector machines (SVM; Vapnik 1995), random forest (RF; Breiman 2001), and ANFIS (Jang 1993). ANN has been utilised in several hydrological processes, including river engineering, water resources management, and hydrology. In terms of accuracy and application, several ANN-based studies have demonstrated an effective method for flow forecast, precipitation prediction, and water quality prediction (Fan et al. 2019; Huang et al. 2019; Samantaray et al. 2022a; Ghose and Samantaray 2019; Samantaray and Ghose 2019; Samantaray et al. 2022b). Several studies have reported application of ANN-based flood prediction models using different meteorological parameters of the study region (Mandal et al. 2005; Han et al. 2007; Dawson et al. 2006; Do Hoai et al. 2011; Elsafi 2014; Mitra et al. 2016; Tsakiri et al. 2018; Sahoo et al. 2022a, b). Singh (2012) applied wavelet-based ANN model for predicting flood events and compared it with existing statistical models. They found that WANN model predicted better flood values than statistical models. In another study, Dhunny et al. (2020) studied the use of ANN model for flood prediction using 20,000 climatic datasets (minimum temperature, maximum temperature, rainfall, and humidity) that were gathered over the course of 2 years for Mauritius. They found ANN to be a good predictor for the specified study region.

Although the ANN method is widely used, it may not produce extremely accurate results, which leads to instability. The inability of ANNs to accurately forecast changes in hydrological variables led to the development of ANFIS that can operate with non-linear relationships. Data pre-processing techniques are required to boost ANN performance. ANFIS is said to be a good amalgamation of ANN and FL. Even though ANN and ANFIS have a lot in common in their modelling stages, reports recommend that ANFIS usually has superior performance than ANN (Sahoo et al. 2022b; Samantaray et al. 2022c; Akrami et al. 2013; El-Shafie et al. 2011); hence, it appears to be a reasonable indication for focusing on ANFIS. It is known to be one of the most beneficial and has a satisfactory performance in modelling many hydrological and environmental phenomena (Kheradpisheh et al. 2015; Mekanik et al. 2016).

Nayak et al. (2005) explored the potential of ANFIS for forecasting flood flow of Kolar river basin, India. In another study, Ullah and Choudhury (2010) explored the usability of ANFIS in flood discharge forecasting of Barak river basin. Both the studies concluded that ANFIS provided better results compared to the ANN model. Nguyen and Chua (2012) implemented ANFIS for daily water level forecasting of Lower Mekong River using water levels of 1 to 5 days ahead. Ghalkhani et al. (2013) used ANN and ANFIS, for flood routing based on different lag times in Madarsoo river basin, Iran. Applied models generated good results at the study location. Anusree and Varghese (2016) applied multiple nonlinear regression (MNLR), ANN, and ANFIS to predict daily flow with different input combinations at exit of Karuvannur river basin. The outcomes indicated that ANFIS predicted river flow more precisely than MNLR and ANN models. Tabbussum and Dar (2021) applied ANN, ANFIS, and fuzzy logic techniques based on different training algorithms to forecast Q_{FD} inflowing Srinagar city at Padshahi Bagh station of Jhelum River. They found that ANFIS model utilising hybrid training algorithm generated best prediction outcomes.

While classic AI techniques are utilised to model different phenomena, they generally suffer from certain shortcomings, such as utilising local search techniques, getting trapped in local optima, high computing, and over-fitting (Kisi et al. 2018; Peyghami and Khanduzi 2013). ANN and ANFIS are two well-known methods utilised for stimulating different hydrological phenomena. Often, they produce satisfactory performance in modelling the events mentioned above; however, they sometimes face problems estimating flood discharge. It may be because the non-linear and non-stationary condition of flow makes its modelling difficult. Hence, it appears to be a good indication to develop modelling quality by diminishing the complications of classical models. But, even though ANFIS has several benefits, its training approaches undergo a few flaws resulting in the incompetence of the models in some circumstances (Kisi et al. 2017). Finding an appropriate structure and its constraints in a neuro-fuzzy (NF) system is essential and also, the system's success depends on its training algorithm's accuracy and efficiency.

Several researches have been published on the successful use of genetic algorithm (GA) in combination with ANN and ANFIS models in predicting river flow discharge (Mukerji et al. 2009; Chau et al. 2005; Wu and Chau 2006). In a similar manner, hybrid ANFIS model with different evolutionary algorithms (Firefly Algorithm (FA); ant colony optimisation (ACO); Whale Optimisation algorithm (WOA); Gray Wolf Optimisation (GWO); Salp Swarm algorithm (SSA); Harris Hawks Optimization (HHO); Butterfly Optimization

Algorithm (BOA); Black Widow Optimization Algorithm (BWOA)) have been successfully applied for modelling several hydrological variables like precipitation, temperature, solar radiation, evapotranspiration, runoff, drought, water table depth, and humidity (Tao et al. 2018; Yaseen et al. 2018; Dehghani et al. 2019; Seifi et al. 2020; Penghui et al. 2020; Samantaray et al. 2022d, e; Panahi et al. 2021; Emami and Emami 2021; Mirboluki et al. 2022, Fadaee et al. 2022). Azad et al. (2018) utilised ACO, GA, and PSO, to train ANFIS for estimating the river flow of Zayandehrood river basin, Iran. Among all considered models, ANFIS-PSO performed best and classical ANFIS performed worst. Yaseen et al. (2019) investigated the potential of GA, PSO, and differential evolution (DE) in tuning membership function (MF) of ANFIS for improving accuracy of streamflow forecasting in River Pahang, Peninsular Malaysia. Analysis of performance indicated that PSO improved the proficiency of ANFIS more than DE and GA algorithms. Inyang et al. (2020) applied k-means, self-organising maps (SOM), ANFIS-GA, and ANFIS-PSO models for predicting flood severity levels. ANFIS-PSO model with lowest error established to be superior compared to other applied models. Arya Azar et al. (2021) evaluated ANFIS, least-squares support vector machine (LS-SVM), and ANFIS-HHO models for predicting evaporation utilising data related to Doroudzan dam located in central Iran. They reported that ANFIS-HHO model gave superior performance to LS-SVR and ANFIS models. Mohammadi et al. (2021) investigated performance of single Non-Recorded Catchment Areas (NRECA), Hydrologiska Byråns Vattenbalansavdelning (HBV), SVM, ANFIS, GMDH (group method of data handling) models, and hybridised NRECA and HBV with ANFIS, SVM, and GMDH models in streamflow prediction considering precipitation and streamflow data of four stations in Indonesia. The results revealed that hybrid models performed better than single models, with hybrid GMDH model performing best among all. Haznedar and Kilinc (2022) developed a hybrid ANFIS-GA model to predict river flow from data collected from Zamanti and Körkün stations of River Seyhan, Turkey, and compared its results with traditional ANN and LSTM models. Their outcomes showed that projected ANFIS-GA technique was successful in predicting river flow more accurately. Malik et al. (2022) applied three machine learning models namely MLP, SVM, and ANFIS and their optimisation with PSO, SMA, and spotted hyena optimiser (SHO) algorithms to predict soil temperature at different depths for a semi-arid zone of Punjab, India. They found that SMA algorithm best optimised the ML models and can be applied for other regions across India.

The developed technique, called ANFIS-PSOSMA, works by constructing a group of solutions, each of which refers to arrangement from ANFIS model's parameters. The training set, representing 70% of total samples, is used to evaluate each solution. The solution with the smallest fitness value is the best, which is found by calculating the RMSE. After that, PSO's operators are utilised for enhancing the existing population. This procedure is trailed by utilising SMA's operators to improve solutions till they attain the final condition. The preeminent arrangement of ANFIS, i.e. the preeminent solution, is assessed utilising a testing set representing 30% of the entire samples. To the best of the authors' understanding, this is the first application of PSOSMA to improve prediction capability of ANFIS and implemented in a real dataset (i.e. flood discharge dataset of Brahmani River). Study flow chart with methodology is given in Fig. 1.

Study area

River Bramhani is the second longest river in Odisha and a major seasonal river in eastern India. The Brahmani is a significant seasonal river in the eastern Indian state of Odisha (Fig. 2). The Sankh and South Koel rivers meet to form the Brahmani, which flows through the Sundargarh, Deogarh, Angul, Dhenkanal, Cuttack, Jajapur, and Kendrapara districts. The basin is located on the right by Mahanadi basin and on the left by Baitarani basin. It forms a sizable delta with the river Baitarani before draining into the Bay of Bengal at Dhamra. It is situated amid 20°30′10″ and 23°36′42″N latitudes and 83°52′55″ and 87°00′38″E longitudes. About 80% of the water of river Bramhani is used in irrigation. In the summer, the temperature may get as high as 47° C, while in the winter, it can get as low as 4 °C. In the state of Odisha, the basin is the primary source of water supplies for several towns and businesses as well as for agriculture. Having a total 39,313.50 km^2 catchment area, it spreads over Chhattisgarh (3.5% of basin area), Jharkhand (39.2% of basin area), and Odisha (57.3% of basin area) states. Flood is a common aspect in Baitarani basin.

Materials and methods

ANN

ANNs have been increasingly utilised in hydrological modelling, like streamflow modelling, rainfall-runoff modelling, and reservoir modelling (Othman and Naseri 2011). ANNs are parallelly dispersed processing systems having tendency of storing experiential information (Latt and Wittenberg 2014). ANN descend connotation from historical dataset, as opposed to physical aspects of a watershed (Cai et al. 2009). MLP is a broadly utilised ANN comprising of neurons called perceptron (Mukerji et al. 2009). In mathematical terms, MLP can be expressed by Eq. (1):

Fig. 1 Study flow chart with methodology

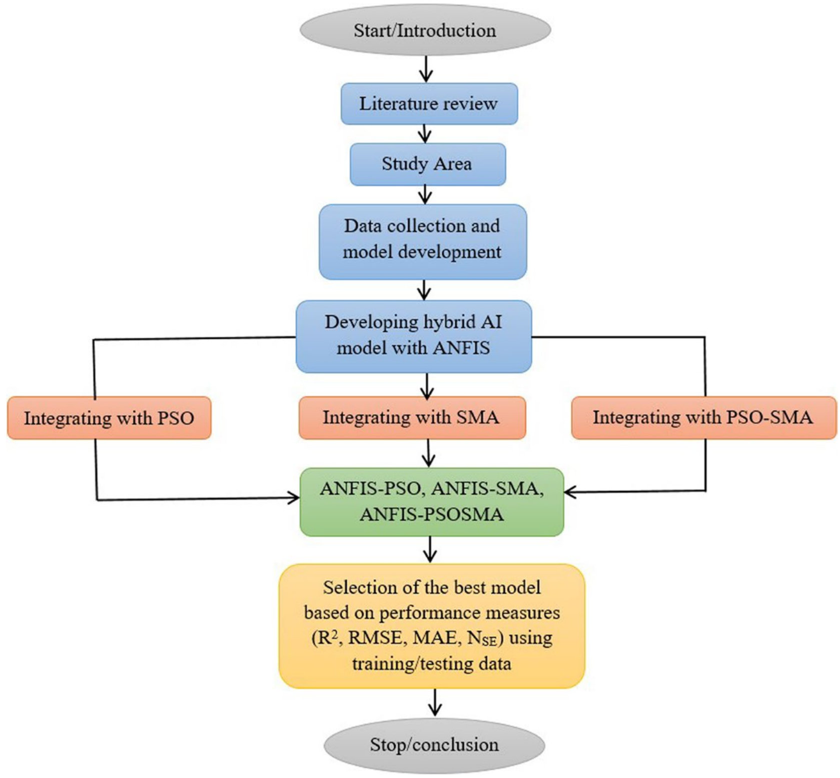

$$y = f(\sum_{z=1}^{n} m_z x_z + b)s \quad (1)$$

where y—output; x_z—input vector ($z = 1 \ldots n$); f—transfer function; m_z—weight vector; b—bias. Basic architecture of ANN is shown in Fig. 3.

ANFIS

A NF system combines ideas of ANNs and fuzzy logic. Depending on training data, they change the types of membership fuzzy functions and inference fuzzy rules using an artificial neural network's learning capability (Das et al. 2019; Sarkar et al. 2021). Learning and logical inference benefits are therefore incorporated into a single system. ANFIS is one of the most widely utilised NF systems (Samantaray et al. 2022g). A multilayer neural network called ANFIS produces output variable's specific value for identified inputs depending on datasets (input–output vector) used during training.

The ability of ANFIS to accurately simulate non-linear links between input and output is a key characteristic. The implementation of an error propagation backward technique, either separately or in conjunction with approach of least squared error, is the foundation of ANFIS training. For describing ANFIS's structure, the system comprises two inputs (x and y), two Sugeno's type fuzzy if–then rules, and a single output (y):

$$Rule\ 1: if(x_1\ is\ C_1)and(x_2\ is\ D_1)then f_1 = p_1x_1 + q_1x_2 + r_1$$
$$Rule\ 1: if(x_1\ is\ C_2)and(x_2\ is\ D_2)then f_2 = p_2x_1 + q_2x_2 + r_2$$

where C_i and D_i—fuzzy sets, q, p, r—subsequent model parameters assessed during training phase. Five layers of the ANFIS structure are seen in Fig. 4.

The 1st layer comprises fuzzy MFs having output function for every node as shown in Eqs. (2) and (3):

$$O_i^1 = \mu_{C_i}(x), i = 1, 2 \quad (2)$$

$$O_i^1 = \mu_{D_{i-1}}(x), i = 3, 4 \quad (3)$$

where μ—generalised Gaussian MF.

The 2nd layer calculates firing power of a rule utilising multiplication operator using Eq. (4):

$$O_i^2 = w_i = \mu_{C_i}(x) \bullet \mu_{D_i}(x), i = 1, 2 \quad (4)$$

The 3rd layer normalises firing power of each rule, utilising ratio between firing power of i th node and addition of firing powers from all nodes (Eq. (5)). Non-adaptive nodes are present in the 3rd layer.

$$O_i^3 = \overline{w_i} = \frac{w_i}{w_1 + w_2}, i = 1, 2 \quad (5)$$

w_i − ith output from layer 2

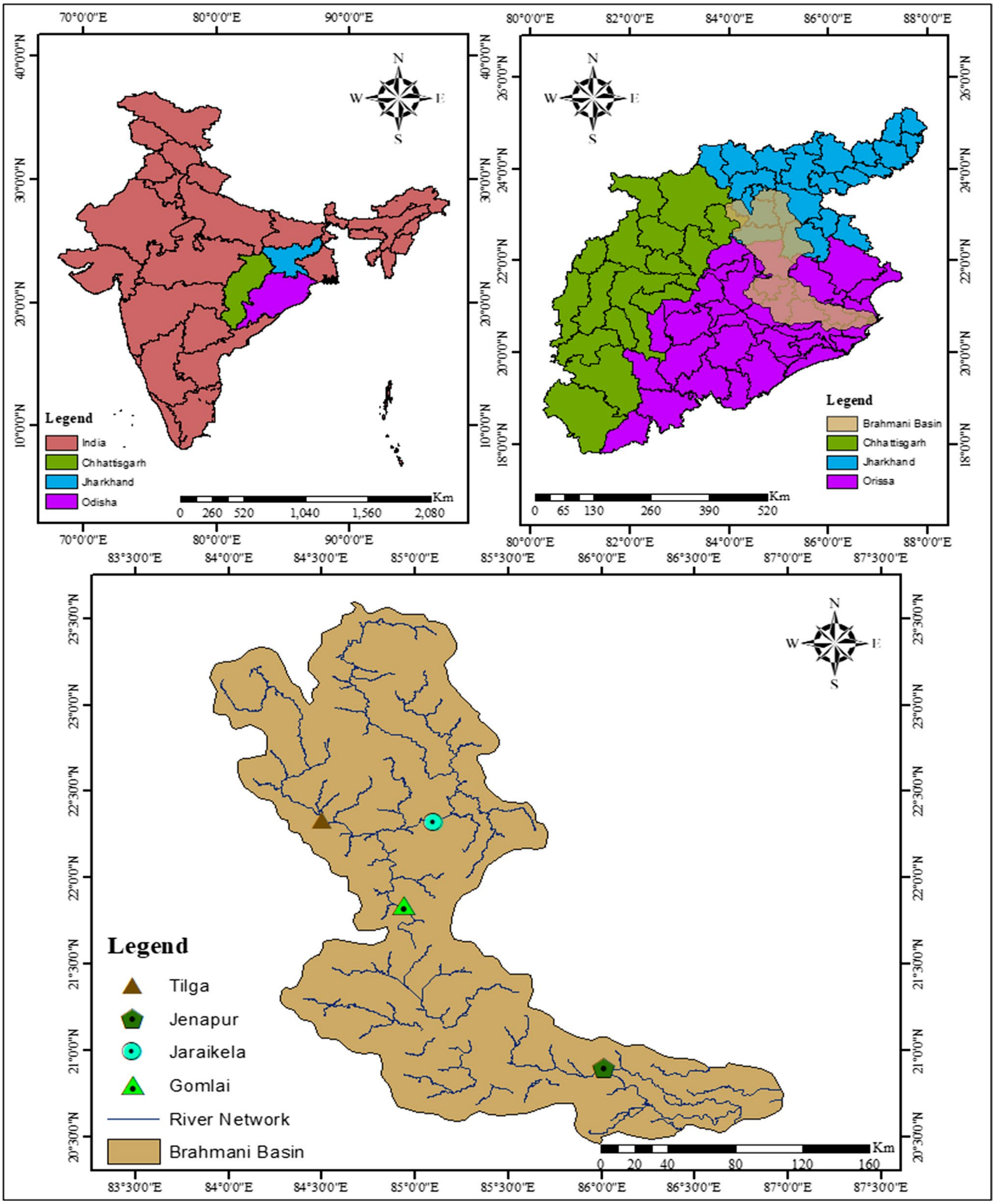

Fig. 2 Study area depicting four selected gauge stations

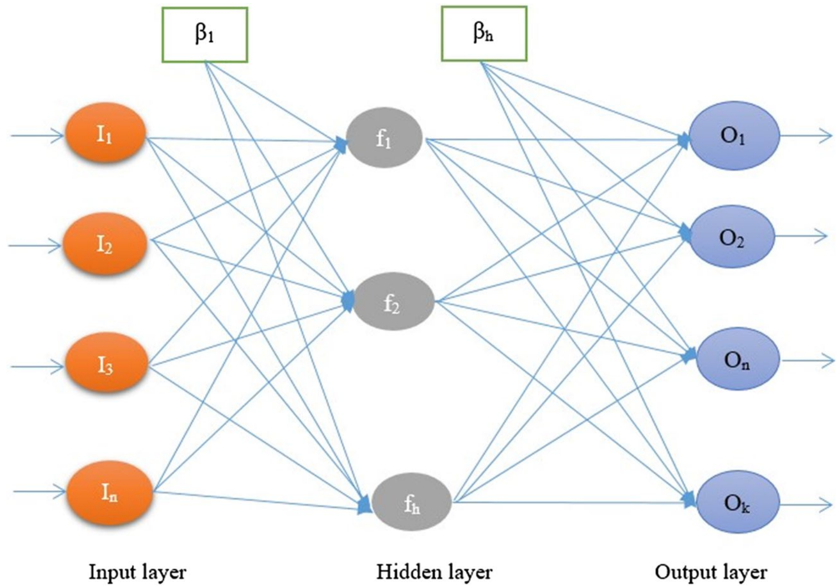

Fig. 3 Architecture of ANN

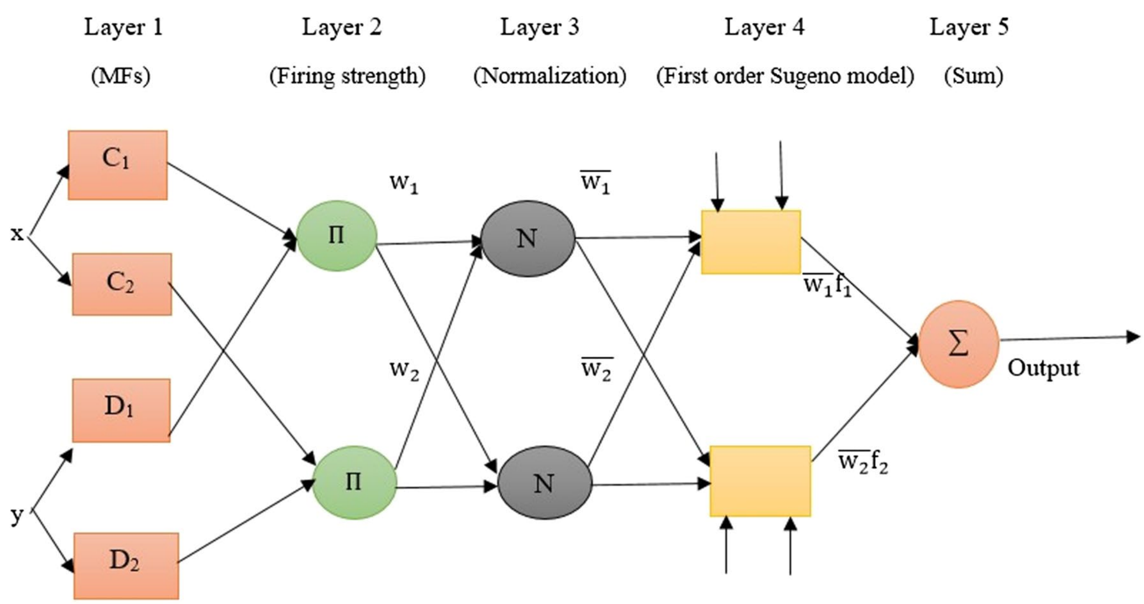

Fig. 4 Architecture of ANFIS

The 4th layer utilises a nodal function for calculating the impact of i th rule concerning the output of the model (Eq. (6)):

$$O_i^4 = \overline{w_i}\left(p_i x + q_i y + r_i\right) = \overline{w_i} f_i \tag{6}$$

where p_i, q_i, and r_i—parameter sets of node and w_i—normalised firing power of 3rd layer.

The 5th layer consists of a solitary non-adaptive node that computes ANFIS model's overall output utilising a summation system (Eq. (7)):

$$O_i^5 = \sum_i \overline{w_i} f_i = \frac{\sum_i w_i f_i}{\sum_i w_i} \tag{7}$$

PSO

Kennedy and Eberhart (1995) proposed a population-based meta-heuristic algorithm known as PSO algorithm for solving optimisation problems. The societal behaviour of cluster of "birds" (particles) inspired the two scientists for developing this optimisation technique. The behaviour of birds

Algorithm 1 PSO algorithm

1. Initialisation of swarm size, position, and velocity of all particles randomly
2. Compute the fitness of each swarm
3. **Do**
4. Compute fitness value of each particle
5. If fitness value is superior than *pbest* fix present value as new *pbest*
6. **End**
7. If fitness value is superior than *gbest* **then** select *gbest* as fitness value as among all particles
8. **End**
9. Update position of each particle using Eq. 8
10. Compute velocity of each particle using Eq. 9
11. **End**
12. While minimum error criteria or maximum iterations are not reached

known as flocking is based on finding certain foodstuff for themselves. At first, population (particle) is initialised by some arbitrarily produced location values. The preeminent position of every particle (*pbest*) is uninterruptedly stored locally in conjunction with the knowledge about global best particle (*gbest*). The position and velocity of all population are updated utilising Eq. 8 and Eq. 9 respectively.

$$x_{i,n}^{j+1} = x_{i,n}^{j} + v_{i,n}^{j+1} \tag{8}$$

$$v_{i,n}^{j+1} = wv_{i,n}^{j} + c_1 r_1 p_{i,n}^{j} - x_{i,n}^{j} + c_2 r_2 p_{g,n}^{j} - x_{i,n}^{j} \tag{9}$$

where $x_{i,n}^{j}$ and $v_{i,n}^{j}$—position and velocity of i^{th} particle respectively, w—inertial weight of current particle utilised for modifying subsequent group of particles, $p_{i,n}^{j}$—personal preeminent location having fitness cost (value) of i th particle usually termed *pbest*, $p_{g,n}^{j}$—global preeminent particle position usually termed *gbest*, c_1 and c_2—coefficient of acceleration utilised for handling exploration and exploitation ability respectively, r_1 and r_2—equally dispersed arbitrary number between [0, 1]. All elements work together with one another to search for a best solution with their optimal fitness function. Basic architecture of PSO is shown in the following algorithm.

SMA

Because metaheuristic algorithms perform better than deterministic algorithms and use less processing power and time, they have gained popularity in several practical fields in recent years. In addition, certain deterministic algorithms are affected by local optima because they lack unpredictability in their latter stages. In contrast, random elements in MAs might cause the algorithm to search for all optimal solutions in the search space, successfully avoiding local optimum. Li et al. (2020) developed a technique for creating wireless sensor networks that use two different slime mould tubular networks corresponding to two different regional routing algorithms.

Approach food

For replicating the contraction technique in this approach, following model equations are expressed (Eq. (10)):

$$\overrightarrow{Y(t+1)} = \begin{cases} \overrightarrow{Y_b(t)} + \overrightarrow{vb} \bullet \left(\overrightarrow{W} \bullet \overrightarrow{Y_A(t)} - \overrightarrow{Y_B(t)}\right), r < p \\ \overrightarrow{vc} \bullet \overrightarrow{Y(t)}, r \geq p \end{cases} \tag{10}$$

where $\overrightarrow{vb}$—constraint utilised in $[-a, a]$, $\overrightarrow{vc}$—constraint values that vary from 1 to 0. $t - t_{th}$ iteration,$\overrightarrow{Y_b}$—discrete location of present best,$\overrightarrow{Y}$—position of present solution, $\overrightarrow{Y_A}$ and $\overrightarrow{Y_B}$—two randomly selected solutions, and $\overrightarrow{W}$—weight of current solution. p value is determined as follows (Eq. (11)):

$$p = tanh|S(i) - bestfitness| \tag{11}$$

where$i \in 1, 2, 3, ..., n$, $S(i)$—fitness function of present solution and $\overrightarrow{vb}$ is found using the following expression Eq. (12):

$$\overrightarrow{vb} = [-a, a], a = \operatorname{arctanh}(-(\frac{t}{\max\_iter}) + 1) \tag{12}$$

The $\overrightarrow{W}$ is obtained based on subsequent Eq. (13):

$$\overrightarrow{W(Smellindex(i))} = \begin{cases} 1 + r \bullet \log\left(\frac{bF - S(i)}{bF - wF} + 1\right), condition \\ 1 - r \bullet \log\left(\frac{bF - S(i)}{bF - wF} + 1\right), others \end{cases} \tag{13}$$

where r—arbitrary value between [0, 1], bF—best-attained fitness values, wF—worst-attained fitness values, and *SmellIndex*—organised fitness values.

Wrap food

When food item is satisfied to extend to a location where the quantity of food is fragile, then the importance of that area diminishes, initiating investigators to move their observation towards other areas of food accessibility which are not as important as the food item. To update the locations, the following mathematical expression is used as depicted:

$$\overrightarrow{Y^*} = \begin{cases} rand.(UB - LB) + LB, rand < z \\ \overrightarrow{Y_B(t)} + \overrightarrow{vb} \bullet \left(\overrightarrow{W} \bullet \overrightarrow{Y_A(t)} - \overrightarrow{Y_B(t)}\right), r < p \\ \overrightarrow{vc} \bullet \overrightarrow{Y(t)}, r \geq p \end{cases} \tag{14}$$

where UB and LB—upper and lower boundaries, *rand* and r —arbitrary values between $[0, 1]$, and z is a value of parameter between $[0, 0.1]$.

Grabble food

$\overrightarrow{vb}$—zone of arbitrary numbers between $[-a, a]$, $\overrightarrow{vc}$ lies between $[-1, 1]$. Even though slime mould obtained an enhanced feed source, it still would extend organic material to seek other sites for a superior-class food source instead of investing all of it in a solitary region for discovering a more consistent nutrition source. The mechanism of SMA algorithm is represented in the following algorithm.

Proposed ANFIS-PSOSMA model

The applied algorithm intends at improving the capability of ANFIS model for predicting Q_{FD} by finding its optimal constraints. This is obtained by utilising a novel metaheuristic algorithm called SMA. SMA is dependent on utilising PSO for generating initial population (first generation) as it has the biggest impact on conjunction of solutions concerning optimum solution. The developed model namely ANFIS-PSOSMA, as shown in Algorithm 3, starts by constructing the network that comprises five layers like the conventional ANFIS. After that, the input data is divided into two groups; first set (70% of total data) is utilised for training the network and finding optimal constraints and second set (30% of total data) is utilised for assessing superlative network built utilising PSOSMA. The subsequent procedure is to generate a group of arbitrary solutions and assess superiority of each one for determining best solution in accordance to training set.

Subsequently, solutions are updated utilising PSO operators, and updated population is delivered to SMA algorithm, which means until they reach at end conditions, operators of SMA will be utilised for updating solutions. The best solution of the preeminent ANFIS network is reverted from learning phase. After that, the testing set is utilised for evaluating performance of the best ANFIS model. Steps of ANFIS-PSOSMA model is demonstrated in Fig. 5.

Evaluating standards

R^2 (Sridharam et al. 2021; Chaudhury et al. 2022; Samantaray and Ghose 2022), MAE (Singh et al. 2022; Jamei et al. 2022), and RMSE (Wang et al. 2022; Ehteram et al. 2019) are standard assessment measures for determining the preeminent prediction model (Eq. (15), Eq. (16), and Eq. (17)). Furthermore, the N_{SE} (Patel et al. 2022; Samani et al. 2022) is also utilised to assess the power of the ANFIS-PSOSMA model (Eq. (18)). For the

Algorithm 2 Pseudo-code of SMA

1. Initialisation of the population size, Maximum iteration (M_t) parameters;
2. Initialisation of slime mould position Y_i (i = 1, 2, 3, 4, 5, • • • • • • , n);
3. Initialisation of the *r, z, W* parameters;
4. **t=1**;
5. **While** ($t \leq M_i$)
6. Compute fitness value for all populations (S);
7. Upgrade Prominent Fitness value, Y_b;
8. Compute the value of $\overrightarrow{W}$ by Eq. (13);
9. **for** each search agents update *vb, p, vc*;
10. Upgrade position by Eq. (14);
11. **end for**
12. t=t+ 1;
13. **end while**
14. **Return** Prominent Fitness value, Y_b;

selection of the best model in this research, the criteria is MAE and RMSE are to be minimum and N_{SE}, R^2 must be maximum.

$$= R^2\left(\frac{\sum_{i=1}^{n}(O_i - \overline{O})(P_i - \overline{P})}{\sqrt{\sum_{i=1}^{n}(O_i - \overline{O})^2 \sum_{i=1}^{n}(P_i - \overline{P})^2}}\right)^2 \tag{15}$$

$$RMSE = \sqrt{\frac{1}{n}\sum_{i=1}^{n}(P_i - O_i)^2} \tag{16}$$

$$MAE = \frac{1}{n}\sum_{i=1}^{n}\|P_i - O_i\| \tag{17}$$

$$N_{SE} = 1 - \left[\frac{\sum_{i=1}^{n}(P_i - O_i)^2}{\sum_{i=1}^{n}(O_i - \overline{O})^2}\right] \tag{18}$$

where

P_i predicted value.

O_i observed value.

$\overline{P}$ mean predicted value

$\overline{O}$ mean observed value

The applied models based on different input combinations of meteorological components (precipitation (P_t), temperature (T_t), humidity (H_t), infiltration (I_t), evapotranspiration (ET_t)) are presented in Table 1. The observed rainfall (P_t), average temperature (T_t), mean humidity (H_t), and mean evapotranspiration loss (E_t) data are collected from IMD (Indian Meteorological Department), Pune. Infiltration data is obtained from Soil Water Infiltration Global Database.

Statistical analysis (minimum, maximum, mean, standard deviation, and kurtosis) of considered hydrological parameters (precipitation, humidity, temperature, evapotranspiration loss, and infiltration), for all datasets (training and testing) of all four stations, is conducted in Tables 2, 3, 4, and 5. The obtained

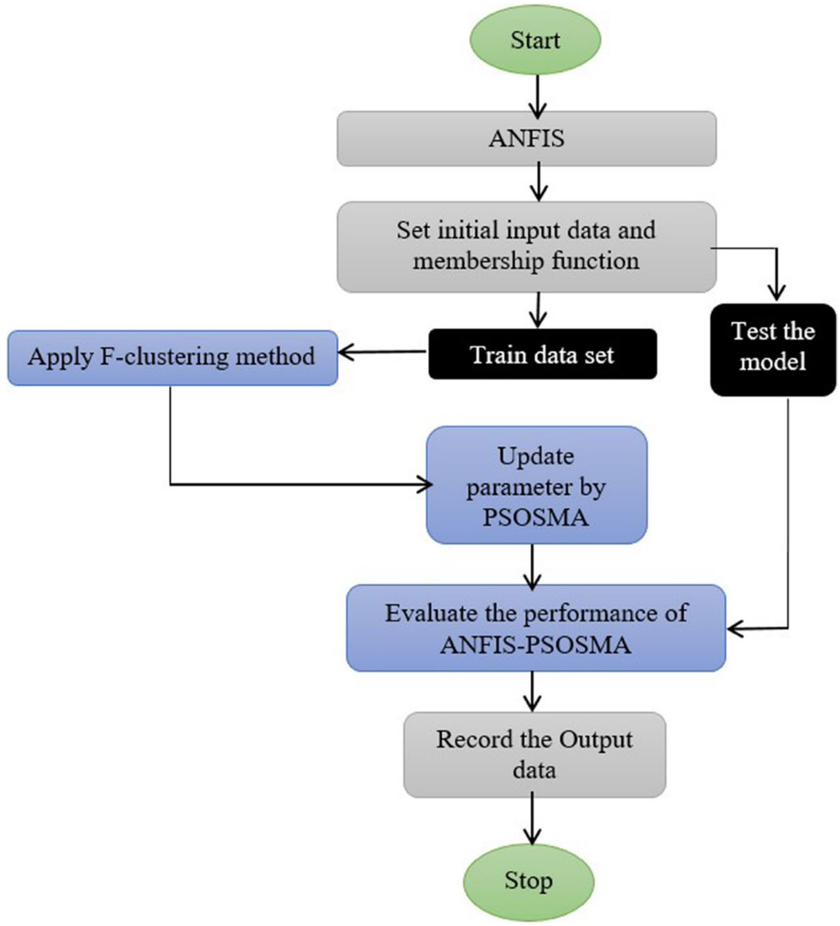

Fig. 5 Steps of ANFIS-PSOSMA

results are presented in Table 6. After monitoring the data quality, datasets were divided into training (70% of complete data) and testing (30% of complete data). The period from January 1990 to December 2010 was utilised to train the models, and from January 2011 to December 2019 to test them.

Results

The performance of three models were tested for predicting monthly Q_{FD} in both training and testing phases utilising different statistical assessment measures (Tables 6, 7, 8, 9, and 10). Based on the applied evaluation measures, it was witnessed that all applied models had good prediction capability ($R^2 > 0.7$). The results of R^2 revealed that applied models are satisfactory; however, ANFIS-PSOSMA model generated the best Q_{FD} values, with the highest value of R^2 (0.9946), followed by ANFIS-SMA (0.9813), ANFIS-PSO (0.9748), ANFIS (0.9657), and ANN (0.9507) models in the training phase and in the testing phase, R^2 values of 0.9731, 0.9517, 0.9436, 0.9314, and 0.9176 in Jenapur station. Considering RMSE values, ANFIS-PSOSMA model had the lowest RMSE (0.0485) proving its best predictive power, followed by ANFIS-SMA (2.2532), ANFIS-PSO (6.8964), ANFIS (13.8749), and ANN (30.9957) models. Moreover, N_{SE} criteria were categorised from highest prediction power to lowest providing similar to R^2, as follows: ANFIS-PSOSMA (0.9952) > ANFIS-SMA (0.9818) > ANFIS-PSO (0.9755) > ANFIS (0.9662) > ANN (0.9513).

The statistical indices discussed above have very well evaluated the prediction capability of projected models. In addition to that, scatter plots and time-series plots are very much useful in assessing the efficiency of forecasting data against the observed data.

It is observed from the scatterplots (Fig. 6) that all models achieved reasonable outcomes in terms of low and high Q_{FD} values. However, the values of R^2 (Fig. 6) showed that ANFIS-PSOSMA performed superiorly compared to other hybrid and conventional models. As shown in Fig. 6d, the outcomes attained from the five models in the Jenapur station are more closely to 45° reference line than those of Jaraikela, Gomlai, and Tilga stations. Also, ANFIS-PSOSMA generated the best R^2 value (0.99468), which inferred superior prediction than other models. The scatter plots of Tilga, Jaraikela, and Gomlai stations are shown in Fig. 6a–c.

Performance of ANN, ANFIS, and ANFIS-SMA are further demonstrated in a more instinctive manner by plotting

Algorithm 3 Pseudo-code of ANFIS-PSOSMA

1. Select and input the dataset
2. State the total number of iterations (t_{max}), maximum epochs, number of solutions (N), increase rate, error goal, initial step, decrease rate.
3. Select input data and break into train (70%) and test (30%) data set
4. Employing FCM clustering to the proposed model
5. Fix the input dataset of membership function
6. Initial population is produced by PSO.
7. **While** (Stopping criteria is not satisfied) **do**
8. Improve the solution using the SMA constraints
9. Calculate the value of fitness function for present scenario.
10. **If** the fitness value is better than the previous one, **then**
11. Save the current value
12. **end if**
13. **end while**
14. Find the Result
15. Stop

observed versus predicted Q_{FD} in the form of hydrographs, as presented in Fig. 6. Monthly forecasting time series data for all models are illustrated in Fig. 6 using data from 1 January 1990 to 31 December 2010 during training, whereas during the testing period uses data from 1 January 2011 to 31 December 2019. For all the stations considered in this study, ANFIS-PSOSMA model performed best for Q_{FD} forecasting, as estimated Q_{FD} values were closer to corresponding actual values and followed similar trend in all sketches, as displayed in Fig. 6. The time-series plots of Tilga, Jaraikela, Gomlai, and Jenapur stations are presented in Fig. 6a–d. Different from predictions from Jaraikela, Gomlai, and Tilga stations, predictions from Jenapur station can better forecast higher and lower flows. Among all the four stations

Table 1 Model scenarios based on different input combinations

Input combinations	Output	Scenario	Model name				
			ANN	ANFIS	ANFIS-PSO	ANFIS-SMA	ANFIS-PSOSMA
P_t	Q_{FD}	I	ANN1	ANFIS1	ANFIS-PSO1	ANFIS-SMA1	ANFIS-PSOSMA1
P_t, T_t		II	ANN2	ANFIS2	ANFIS-PSO2	ANFIS-SMA2	ANFIS-PSOSMA2
P_t, T_t, H_t		III	ANN3	ANFIS3	ANFIS-PSO3	ANFIS-SMA3	ANFIS-PSOSMA3
P_t, T_t, H_t, I_t		IV	ANN4	ANFIS4	ANFIS-PSO4	ANFIS-SMA4	ANFIS-PSOSMA4
P_t, T_t, H_t, I_t, ET_t		V	ANN5	ANFIS5	ANFIS-PSO5	ANFIS-SMA5	ANFIS-PSOSMA5

Table 2 Statistical parameters of applied data Tilga

Statistical parameters	Training set (252)	Testing set (108)	Total data set (360)	Training set (252)	Testing set (108)	Total data set (360)
Precipitation				Humidity		
Min	0	0	0	58.54	59.5	58.54
Max	56.064	47.86	56.06	83.04	83.04	83.04
Mean	40.616	43.762	40.616	71.20175	71.0052	71.14559
Kurt	1.942	1.256	1.317	−0.95765	−0.99391	−0.97411
SD	46.281	46.378	45.519	6.25959	6.59965	6.33928
Skew	1.334	1.128	1.208	−0.0072	0.05259	0.00939
Temperature				Evapotranspiration		
Min	18.5	18.5	18.5	78.54	79.5	78.54
Max	33.5	32.63	33.5	116.88	126.88	126.88
Mean	27.50175	27.14895	27.4009	98.03508	98.5669	98.22505
Kurt	−0.57584	−1.03682	−0.72528	−0.7702	−0.8359	−0.79538
SD	3.3617	3.91405	3.51994	9.187584	9.89156	9.38803
Skew	−0.50559	−0.367	−0.46928	−0.01812	0.01391	0.01115
Infiltration						
Min	4.276	14.469	4.276			
Max	11.478	21.638	21.638			
Mean	7.892	18.335	8.22			
Kurt	0.59	9.414	34.526			
SD	0.758	5.146	2.789			
Skew	0.889	−1.634	−3.9			

considering the five applied models, the prediction accuracy of Jaraikela station is poor with the least R^2 value in both the training and testing stages.

Linear scale plot of actual vs. estimated Q_{FD} for applied models are demonstrated in Fig. 7. The figures demonstrate that predicted peak Q_{FD} are 459.179M^3/s, 454.666M^3/s, 444.198M^3/s, 433.496M^3/s, 414.187M^3/s for ANFIS-PSOSMA, ANFIS-SMA, ANFIS-PSO, ANFIS, and ANN in contrast to actual peak of 465.274M^3/s for Tilga station. The approximated peak discharges are 3736.342M^3/s, 3705.635M^3/s, 3624.51M^3/s, 3541.109M^3/s, and 3344.36M^3/s for ANFIS-PSOSMA, ANFIS-SMA, ANFIS-PSO, ANFIS, and ANN against actual peak 3790.931M^3/s for Jaraikela division. For Gomlai gauging station, actual Q_{FD} is 2859.61M^3/s aligned with predicted Q_{FD} 2822.149M^3/s, 2804.991M^3/s, 2736.075M^3/s, 2667.444M^3/s, and 2547.626M^3/s for ANFIS-PSOSMA, ANFIS-SMA, ANFIS-PSO, ANFIS, and ANN correspondingly. Similarly, for Jenapur, observed peak discharge is 4432.095M^3/s with respect to predicted Q_{FD} 4371.819M^3/s, 4326.168M^3/s, 4242.401M^3/s, 4143.566M^3/s, and 3871.435M^3/s, for ANFIS-PSOSMA, ANFIS-SMA, ANFIS-PSO, ANFIS, and ANN respectively.

The results of boxplot are shown in Fig. 8. The boxplot of ANFIS-PSOSMA model for Q_{FD} prediction was nearly close to the actual boxplot compared to other two hybrid models (ANFIS-SMA and ANFIS-PSO), whereas conventional ANFIS, and ANN underestimated Q_{FD}. In terms of quartile, minimum and median values of all considered models were capable of predicting Q_{FD} values closer to

Table 3 Statistical parameters of applied data Jenapur

Statistical parameters	Training set (252)	Testing set (108)	Total data set (360)	Training set (252)	Testing set (108)	Total data set (360)
Precipitation				Humidity		
Min	0	0	0	56.03	56.03	56.03
Max	64.3	52.709	64.3	84.06	82.83	84.06
Mean	38.558	31.384	30.91	71.9143	70.31995	71.45878
Kurt	1.103	3.953	2.218	−0.61569	−0.70499	−0.6799
SD	1.303	1.854	1.629	6.21456	6.38536	6.28626
Skew	45.519	40.99	43.115	−0.23484	−0.03069	−0.17763
Temperature				Evapotranspiration		
Min	15.998	15.811	15.81	75.63	75.63	75.63
Max	35.49	34.03	35.49	118.54	118.39	118.54
Mean	24.965	24.794	24.95	99.103	98.85047	98.8398
Kurt	−0.908	−0.898	−0.926	−0.60293	−0.5028	−0.65282
SD	4.867	4.896	4.798	9.42552	10.1193	9.71719
Skew	−0.104	−0.222	−0.117	−0.23999	−0.40922	−0.27184
Infiltration						
Min	6.876	7.986	6.876			
Max	12.375	19.912	12.375			
Mean	7.268	16.859	11.69			
Kurt	6.761	7.975	5.253			
SD	1.141	16.71	25.309			
Skew	−6.131	−4.231	−7.031			

Table 4 Statistical parameters of applied data Jaraikela

Statistical parameters	Training set (252)	Testing set (108)	Total data set (360)	Training set (252)	Testing set (108)	Total data set (360)
Precipitation				Humidity		
Min	0	0	0	55.63	55.63	55.63
Max	31.9433	45.01612	45.0161	83.56	80.28	83.56
Mean	14.1022	15.176	14.409	72.2696	70.7339	71.83089
Kurt	−0.23636	4.26539	1.60301	−0.75206	−0.73296	−0.7316
SD	6.4822	7.4039	6.75323	6.40163	6.09722	6.33632
Skew	0.35487	1.19493	0.67883	−0.29777	−0.403	−0.30111
Temperature				Evapotranspiration		
Min	17.604	17.24	17.24	76.03	76.03	76.03
Max	34.195	34.017	34.195	119.06	119.06	119.06
Mean	25.648	25.603	25.78	98.74765	98.72714	98.59665
Kurt	−0.818	−0.851	−0.846	−0.6237	−0.6469	−0.6886
SD	4.247	4.265	4.172	9.18446	10.3923	9.53081
Skew	−0.198	−0.341	−0.217	−0.17516	−0.23558	−0.17209
Infiltration						
Min	5.815	6.964	5.815			
Max	17.478	20.638	20.638			
Mean	12.892	17.335	13.867			
Kurt	0.49	9.314	39.536			
SD	0.678	4.676	3.829			
Skew	0. 909	−1.634	−3.8			

Table 5 Statistical parameters of applied data Gomlai

Statistical parameters	Training set (252)	Testing set (108)	Total data set (360)	Training set (252)	Testing set (108)	Total data set (360)
Precipitation				Humidity		
Min	0	0	0	57.08	58.65	57.08
Max	49.6741	31.5266	49.6741	84.39	80.26	84.39
Mean	13.3295	12.537	13.10319	71.7395	70.2179	71.30476
Kurt	6.51936	1.19518	5.85473	−0.82138	−1.2634	−0.94228
SD	6.8629	5.78952	6.5669	6.48346	6.47202	6.49748
Skew	1.68424	0.3141	1.4461	−0.26771	−0.18937	−0.23853
Temperature				Evapotranspiration		
Min	19.08	19.19	19.08	77.08	78.65	77.08
Max	36.14	34.5	36.14	118.37	119.67	118.37
Mean	27.5395	27.8052	27.6154	98.5728	98.5747	98.39434
Kurt	−0.56664	−0.58996	−0.5996	−0.6147	−0.6779	−0.7053
SD	3.8947	4.1578	3.9609	9.29678	10.32044	9.58354
Skew	−0.2275	−0.41	−0.2778	−0.2543	−0.35306	−0.25636
Infiltration						
Min	4.975	6.134	4.975			
Max	18.375	21.912	21.912			
Mean	9.268	18.637	14.53			
Kurt	5.674	8.673	7.651			
SD	2.346	12.79	13.309			
Skew	−6.57	−3.324	−8.164			

Table 6 Performance of ANN

Station	Scenario	Training				Testing			
		N_{SE}	RMSE	R^2	MAE	N_{SE}	RMSE	R^2	MAE
Tilga	I	0.9355	43.995	0.935	20.368	0.9055	50.7893	0.905	28.6945
	II	0.9381	43.3987	0.9377	20.0919	0.9086	50.219	0.9079	28.3723
	III	0.9403	41.7894	0.9397	23.2163	0.9102	49.662	0.9097	22.2699
	IV	0.942	39.9426	0.9416	19.0202	0.9121	49.284	0.9114	22.1004
	V	0.9439	39.004	0.9434	18.5733	0.9138	49.1102	0.9134	22.0225
Jaraikela	I	0.9344	44.2168	0.9338	20.4707	0.9013	51.228	0.9009	28.9423
	II	0.9365	43.7901	0.9359	20.2731	0.9036	50.9942	0.9031	28.8102
	III	0.9367	43.689	0.936	20.2263	0.9059	50.511	0.9053	28.5372
	IV	0.9393	42.7043	0.9387	23.7246	0.9071	50.3278	0.9065	28.4337
	V	0.9409	41.1085	0.9403	22.838	0.9098	49.921	0.9094	22.3861
Gomlai	I	0.9393	42.4843	0.9389	23.6023	0.91	49.8863	0.9096	22.3705
	II	0.9406	41.5089	0.9402	23.0605	0.9114	49.3116	0.9108	22.1128
	III	0.942	40.3278	0.9414	22.4043	0.9142	48.8897	0.9137	21.9674
	IV	0.9442	38.77	0.9436	18.4619	0.9155	48.6003	0.9149	21.7938
	V	0.9457	37.5245	0.9452	17.8688	0.9167	48.4417	0.9163	21.7227
Jenapur	I	0.9326	44.3775	0.932	20.5451	0.911	49.47	0.9105	22.1838
	II	0.9461	36.8965	0.9455	17.5697	0.9141	48.9874	0.9136	21.9236
	III	0.947	36.258	0.9466	19.4935	0.9154	48.721	0.9148	21.8479
	IV	0.9493	33.7145	0.9489	18.126	0.9166	48.5879	0.916	21.7883
	V	0.9513	30.9957	0.9507	16.6643	0.9181	48.239	0.9176	21.6318

Table 7 Performance of ANFIS

Station	Scenario	Training				Testing			
		N_{SE}	RMSE	R^2	MAE	N_{SE}	RMSE	R^2	MAE
Tilga	I	0.9514	30.2856	0.9509	16.2825	0.9207	47.902	0.9203	27.3725
	II	0.9519	29.8129	0.9513	16.0284	0.9217	47.621	0.9211	27.212
	III	0.9531	28.5436	0.9525	13.3381	0.9238	47.003	0.9234	26.8588
	IV	0.9551	27.2367	0.9547	12.7200	0.9252	46.7884	0.9247	26.7362
	V	0.9571	25.6895	0.9565	12.0044	0.9256	46.6901	0.9250	26.68
Jaraikela	I	0.9477	36.0045	0.9473	19.3572	0.9192	48.1883	0.9186	21.6091
	II	0.9492	34.5147	0.9485	18.5562	0.9205	48.0067	0.9198	21.5276
	III	0.9501	33.4179	0.9495	17.9666	0.9208	47.8219	0.9204	27.3268
	IV	0.9512	30.7128	0.9508	16.5122	0.9221	47.44	0.9216	27.1085
	V	0.9522	29.0048	0.9518	15.5939	0.9238	47.1184	0.9231	26.9248
Gomlai	I	0.9535	28.2149	0.9529	13.1845	0.9226	47.2386	0.9220	26.9934
	II	0.954	27.8214	0.9534	13.0006	0.9246	46.899	0.9241	26.7993
	III	0.955	27.5398	0.9543	12.8690	0.9258	46.5997	0.9252	26.6284
	IV	0.9571	25.9713	0.9565	12.1361	0.9278	45.906	0.9274	26.232
	V	0.9591	25.0174	0.9587	11.6903	0.9289	45.679	0.9283	26.1022
Jenapur	I	0.9625	19.0054	0.9618	9.8986	0.9272	46.421	0.9265	26.5262
	II	0.9624	18.9412	0.962	9.8652	0.9284	45.8742	0.9279	26.2138
	III	0.9637	18.2201	0.9631	9.494	0.9301	45.3216	0.9294	20.9822
	IV	0.9648	15.239	0.9642	8.6371	0.9305	45.1176	0.9300	20.8877
	V	0.9662	13.8749	0.9657	6.6706	0.9319	44.7421	0.9314	20.7139

Table 8 Performance of ANFIS-PSO

Station	Scenario	Training				Testing			
		N_{SE}	RMSE	R^2	MAE	N_{SE}	RMSE	R^2	MAE
Tilga	I	0.9607	23.17	0.96	10.82	0.9352	44.02	0.9348	20.3796
	II	0.9616	21.8631	0.9612	11.387	0.9373	43.5731	0.9369	20.1727
	III	0.964	16.587	0.9633	8.639	0.9392	42.59	0.9388	23.6611
	IV	0.9653	15.0067	0.9647	7.2147	0.9408	41.33	0.9403	22.9611
	V	0.966	14.2587	0.9655	6.8551	0.9421	40.168	0.9414	19.1276
Jaraikela	I	0.9527	29.0048	0.9522	15.59	0.927	46.2296	0.9266	26.4169
	II	0.9552	27.2367	0.9547	12.7274	0.9295	45.4821	0.9289	21.0565
	III	0.9561	26.1785	0.9556	12.2329	0.9305	44.9832	0.9301	20.8255
	IV	0.9581	25.3517	0.9574	11.8465	0.9323	44.589	0.9317	20.643
	V	0.9602	23.5214	0.9596	10.9913	0.9386	43.1832	0.938	19.9922
Gomlai	I	0.9634	18.2291	0.9629	9.4943	0.9387	42.97	0.9381	23.8722
	II	0.9642	16.3201	0.9638	8.5005	0.93979	42.1267	0.9392	23.4037
	III	0.9658	14.7962	0.9652	7.1135	0.94048	41.66	0.94	23.1444
	IV	0.9669	12.8412	0.9664	6.1736	0.94147	40.775	0.941	22.6527
	V	0.9688	12.3541	0.9683	5.9394	0.94323	39.5064	0.9426	18.8125
Jenapur	I	0.970	11.8459	0.9694	5.6951	0.9401	41.8904	0.9395	23.2724
	II	0.9712	10.8746	0.9706	5.5767	0.9407	41.496	0.9402	23.0533
	III	0.973	9.0215	0.9723	4.6264	0.9416	40.621	0.941	22.5672
	IV	0.9734	8.8147	0.973	4.5203	0.9434	39.337	0.9427	18.7319
	V	0.9755	6.8964	0.9748	3.5366	0.9441	38.915	0.9436	18.5309

actual values with a substantial degree of precision, even though ANFIS-PSOSMA model performed best among all models.

Correspondingly, frequency analysis is done through a histogram plot (Fig. 9) of actual and predicted data set. The *x*-axis presents Q_{FD} values, and the number of events

Table 9 Performance of ANFIS-SMA

Station	Scenario	Training				Testing			
		N_{SE}	RMSE	R^2	MAE	N_{SE}	RMSE	R^2	MAE
Tilga	I	0.9727	10.125	0.9722	5.1923	0.941	41.003	0.9404	22.7794
	II	0.9741	8.1285	0.9736	4.1684	0.9417	40.4492	0.9411	22.4717
	III	0.9756	6.721	0.9751	3.4466	0.9431	39.2964	0.9427	18.7125
	IV	0.978	5.4985	0.9773	2.6953	0.946	37.524	0.9455	17.86
	V	0.9795	4.9935	0.979	2.4477	0.948	35.7136	0.9474	19.2008
Jaraikela	I	0.9702	11.5698	0.9698	5.5624	0.939	42.8862	0.9384	23.8256
	II	0.9705	11.3652	0.97	5.46403	0.9396	42.338	0.9391	23.5211
	III	0.9716	10.498	0.971	5.3835	0.941	40.9012	0.9405	22.7228
	IV	0.9728	9.4215	0.9722	4.8315	0.9456	38.189	0.9449	18.1852
	V	0.9744	7.8863	0.9739	4.0442	0.947	36.5412	0.9464	19.6458
Gomlai	I	0.9751	7.0245	0.9745	3.6023	0.9431	39.71	0.9426	18.9095
	II	0.9757	6.5418	0.9752	3.3547	0.9454	38.4286	0.9448	18.2993
	III	0.977	6.0469	0.9764	3.1009	0.9465	36.789	0.9459	19.779
	IV	0.9807	4.3641	0.9801	2.1392	0.9488	34.8356	0.9482	18.7288
	V	0.9807	3.0589	0.9803	1.4994	0.9511	32.1456	0.9505	17.2825
Jenapur	I	0.9767	6.2483	0.9762	3.2042	0.9454	37.9006	0.9450	18.0479
	II	0.9776	5.8463	0.977	2.8658	0.9486	35.1149	0.9481	18.8789
	III	0.979	5.238	0.9786	2.5676	0.9502	32.8145	0.9497	17.6422
	IV	0.9807	3.6214	0.9804	1.7751	0.9508	32.4239	0.9503	17.4322
	V	0.9818	2.2532	0.9813	1.1045	0.9524	29.4398	0.9517	15.8278

Table 10 Performance of ANFIS-PSOSMA

Station	Scenario	Training				Testing			
		N_{SE}	RMSE	R^2	MAE	N_{SE}	RMSE	R^2	MAE
Tilga	I	0.9817	2.5574	0.9812	1.2536	0.9601	23.8419	0.9596	11.141
	II	0.9828	2.0482	0.9821	1.004	0.9611	22.5418	0.9607	10.5335
	III	0.9856	1.7312	0.9851	0.8487	0.9625	19.4957	0.9618	10.154
	IV	0.988	0.3157	0.9875	0.1725	0.9665	13.4128	0.9659	6.4484
	V	0.9908	0.2034	0.9901	0.1111	0.9694	12.3532	0.9688	5.939
Jaraikela	I	0.9791	5.0147	0.9787	2.4581	0.9595	24.3974	0.959	11.4006
	II	0.9805	4.7548	0.9799	2.3307	0.9606	23.174	0.96	10.8289
	III	0.9815	2.7846	0.981	1.365	0.9622	20.3674	0.9617	10.608
	IV	0.9845	1.7314	0.9841	0.8487	0.9645	15.5217	0.9639	8.0842
	V	0.9872	0.7942	0.9865	0.4339	0.9657	14.5239	0.9653	6.9826
Gomlai	I	0.9836	1.9523	0.9829	0.957	0.9619	21.4125	0.9614	11.1523
	II	0.9864	0.9007	0.985	0.4921	0.9643	16.3211	0.9639	8.5005
	III	0.9878	0.5345	0.9874	0.292	0.9669	13.1987	0.9662	6.3455
	IV	0.991	0.1995	0.9903	0.109	0.9685	12.6587	0.968	6.0859
	V	0.9931	0.1541	0.9926	0.0842	0.9714	10.494	0.9708	5.383
Jenapur	I	0.9895	0.2846	0.9889	0.1555	0.9663	13.5147	0.9658	6.4974
	II	0.9906	0.2462	0.99	0.1345	0.9695	12.3541	0.9689	5.9394
	III	0.9922	0.1993	0.9918	0.109	0.9707	11.2147	0.9702	5.3916
	IV	0.9942	0.0967	0.9937	0.0528	0.9722	10.121	0.9718	5.192
	V	0.9952	0.0485	0.9946	0.0265	0.9736	8.4236	0.9731	4.3197

was determined by the bin ranges of the histograms. From the above analysis, it is clearly found that ANFIS-SMA is more suitable than ANFIS and ANN approach. It can be concluded that after incorporating SMA to ANFIS models, there is a noticeable decrease in forecasting uncertainty resulting in the assessment of the prediction model.

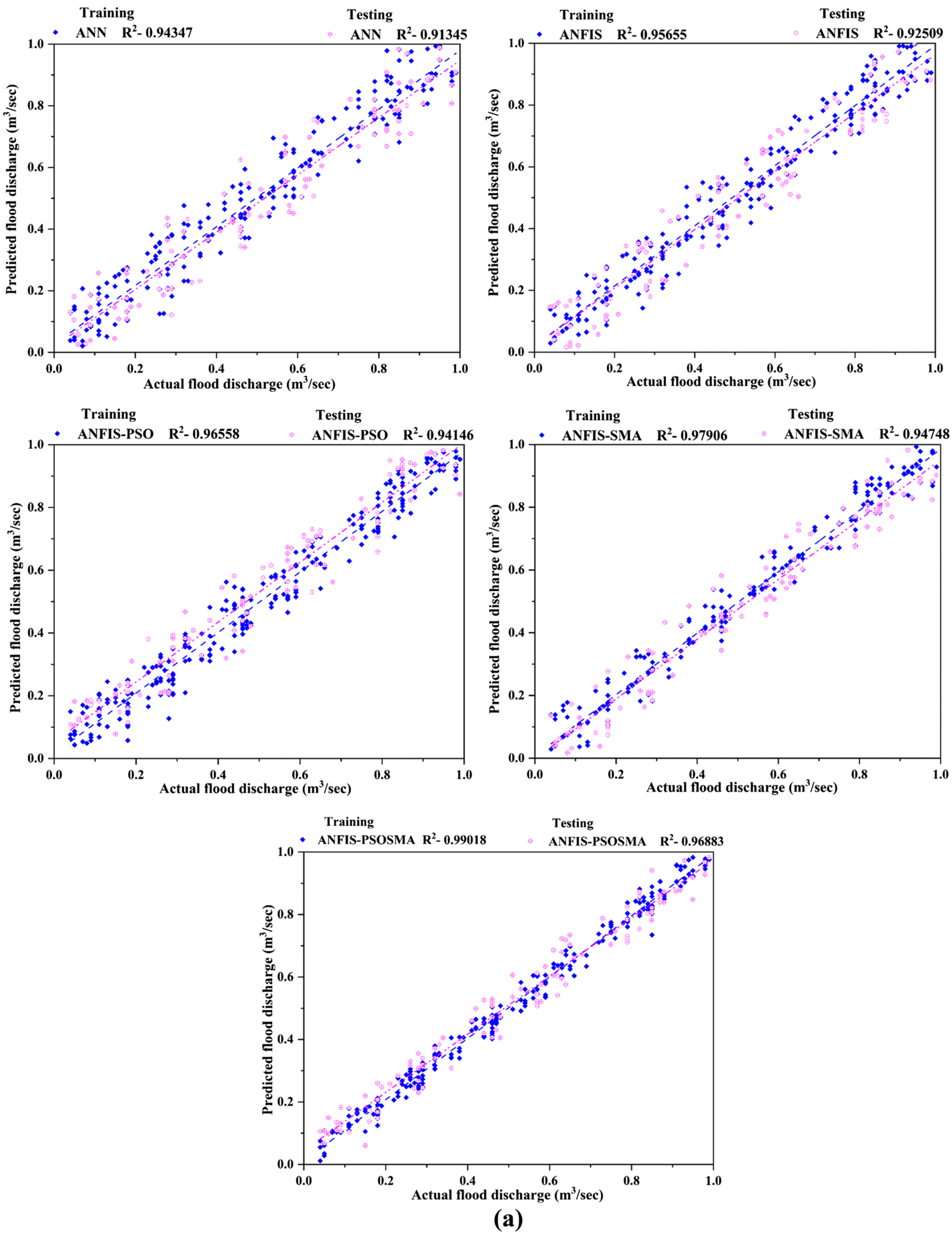

Fig. 6 Scatter plots of actual vs. predicted flood discharge using ANN, ANFIS, ANFIS-PSO, ANFIS-SMA, and ANFIS-PSOSMA models for **a** Tilga, **b** Jaraikela, **c** Gomlai, and **d** Jenapur stations

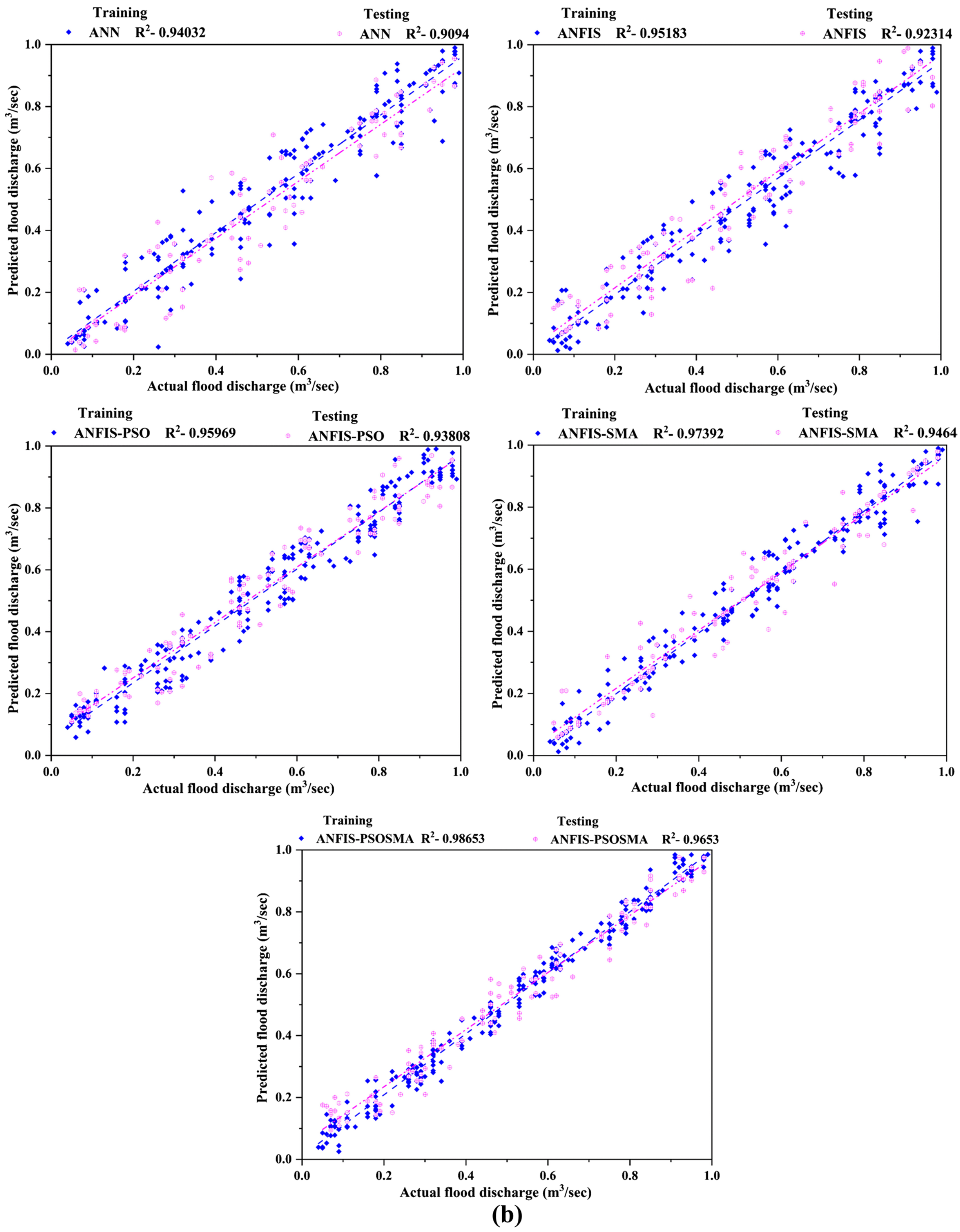

Fig. 6 (continued)

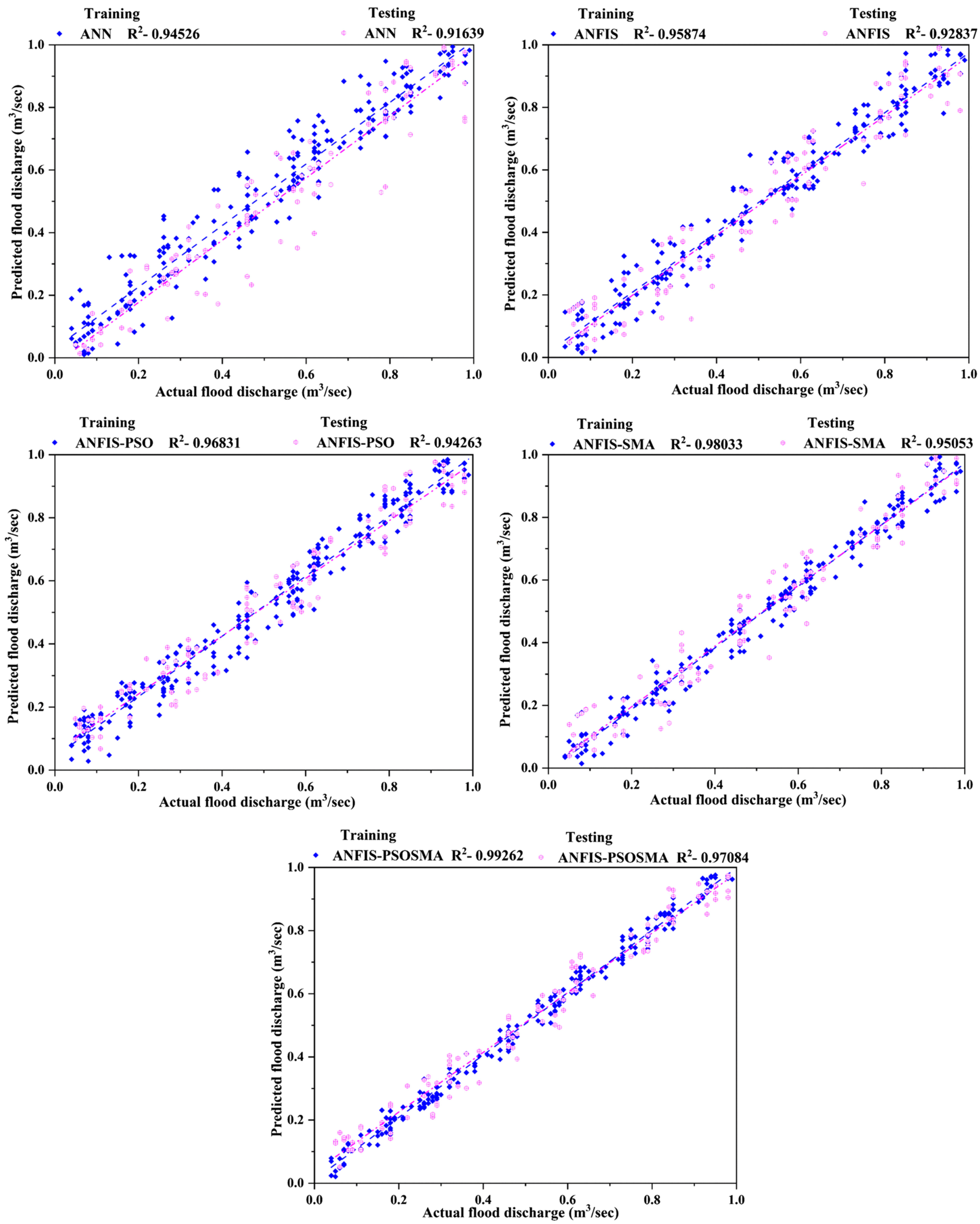

(c)

Fig. 6 (continued)

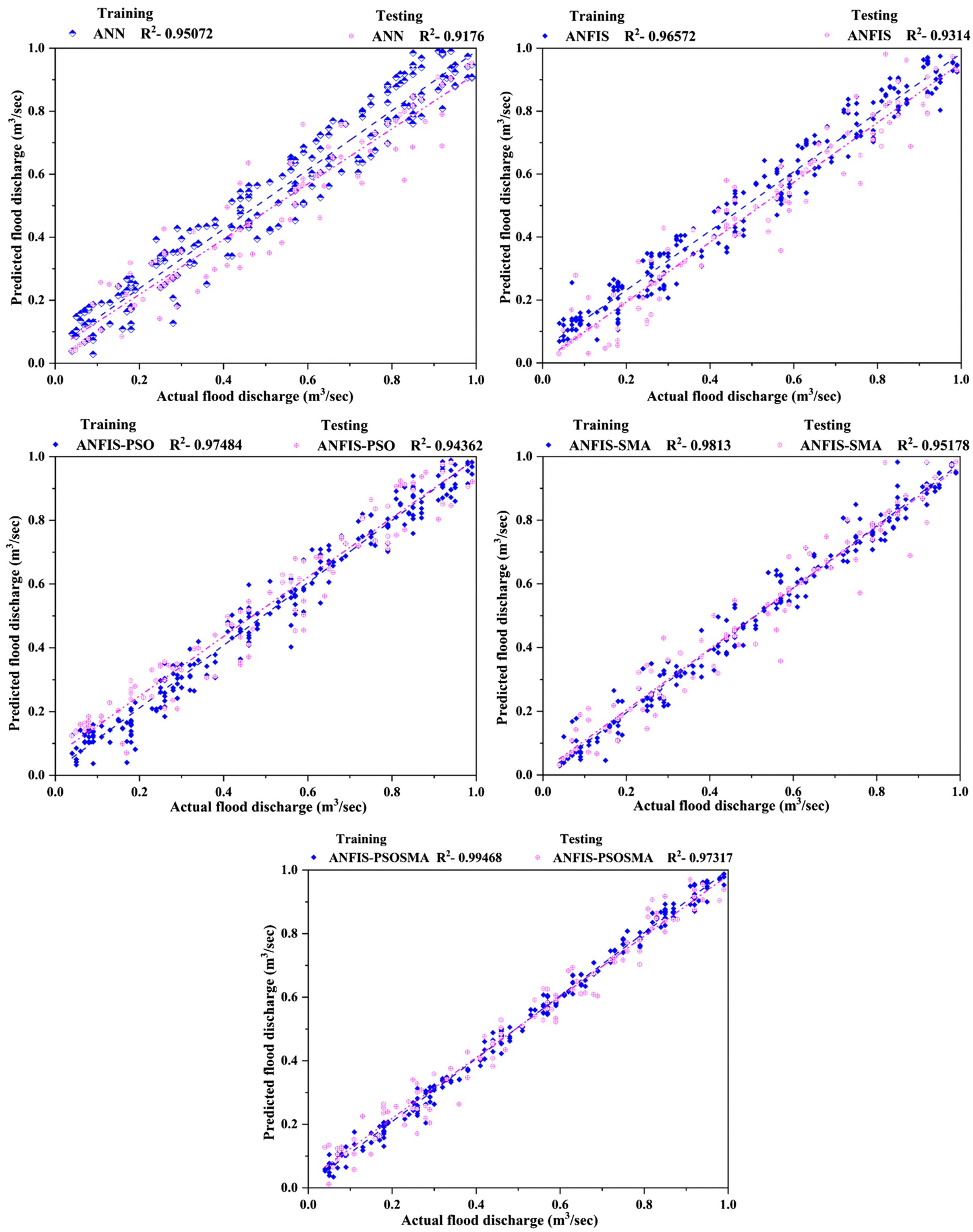

(d)

Fig. 6 (continued)

Fig. 7 Observed and computed stream flow for **a** Tilga, **b** Jaraikela, **c** ▶ Gomlai, and **d** Jenapur stations

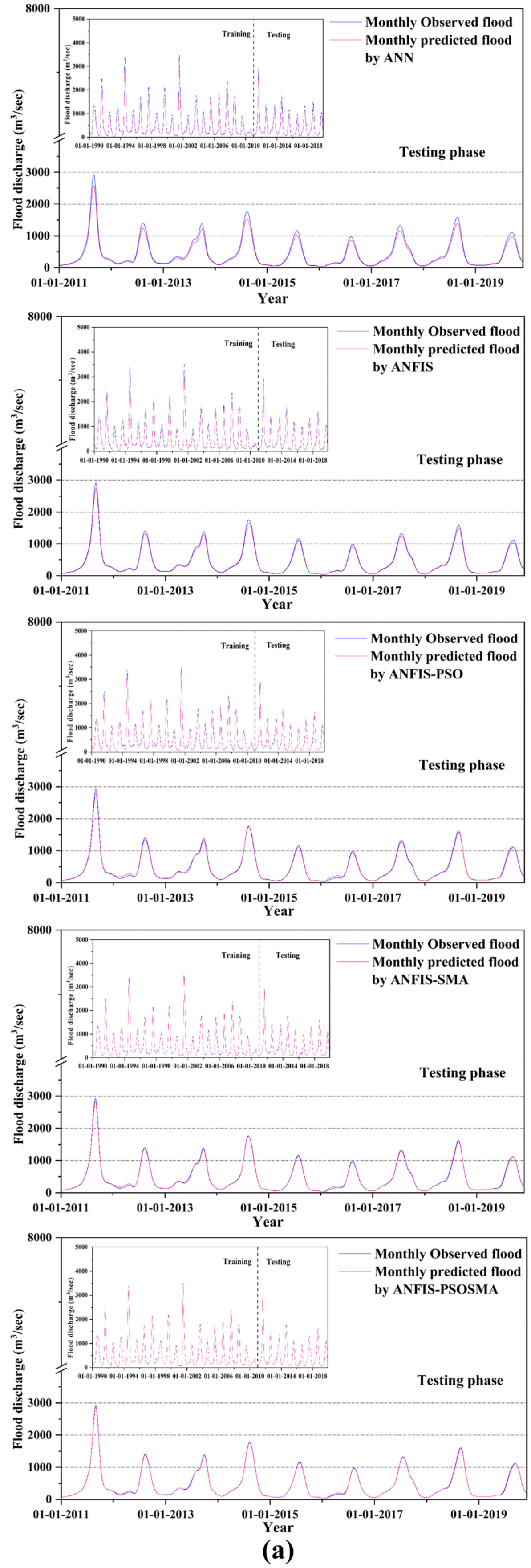

Discussion

The applied models realise flood discharge prediction with a forecasting horizon. The performance criteria of hybrid ANFIS-PSOSMA is satisfactory (NSE = 0.9952, RMSE = 0.0485 R^2 = 0.9946, MAE = 0.0265). The coefficient of determination (Fig. 6) illustrates that the developed model has adequately acquired the aspects of time series (Q_{FD}) of training data series. The predicted and observed Q_{FD} by ANFIS-PSOSMA model are nearly similar (Fig. 7). The same situation is observed with the NSE (0.9952). A small deviation is observed in terms of the RMSE (0.0485) between the forecasted flood discharge against the actual discharge. Hence, the proposed hybrid ANFIS-PSOSMA model has appropriately adjusted with variations in the input dataset (meteorological components) during the training period. The evaluation of generalisation capability, i.e. absence of overfitting or underfitting, is conducted with the testing dataset which has not been utilised in the training period. For each occurrence, testing results showed a good generalisation capability of the selected model. This reveals that there was neither overfitting nor underfitting during training. Also, it specifies perfect forecasts of flood peaks. There was a slight deviation between predicted and observed flood peaks, and hence, we can conclude that ANFIS-PSOSMA model has a better forecasting or prediction ability for flood peaks. The major advantage of the developed holistic approach is automatic determination of ANFIS variables and arrangement of key standardisation samples for overcoming limitations of conventional ML in modelling real-world problems when series of sample values is huge. The PSO is utilised for modifying search operators of SMA for avoiding its limitations in determining preeminent solution because of its fragile exploitation capability. As a result, integration of PSO and SMA, i.e. PSOSMA, utilises benefits of both SMA and PSO, and it shows higher performance outcomes compared to original SMA and PSO.

The key drawback of this research is the assessment of five applied ML approaches utilising data from a particular area. The proposed techniques can further be verified by utilising additional data from other climatic conditions. Also, the prospective of hybridisation of PSOSMA technique with stochastic models, mainly models with exogenous input, necessities to be evaluated. In future works, integrating ANFIS-PSOSMA with ensemble modelling techniques (like Bayesian model averaging) or preprocessing methods (e.g.

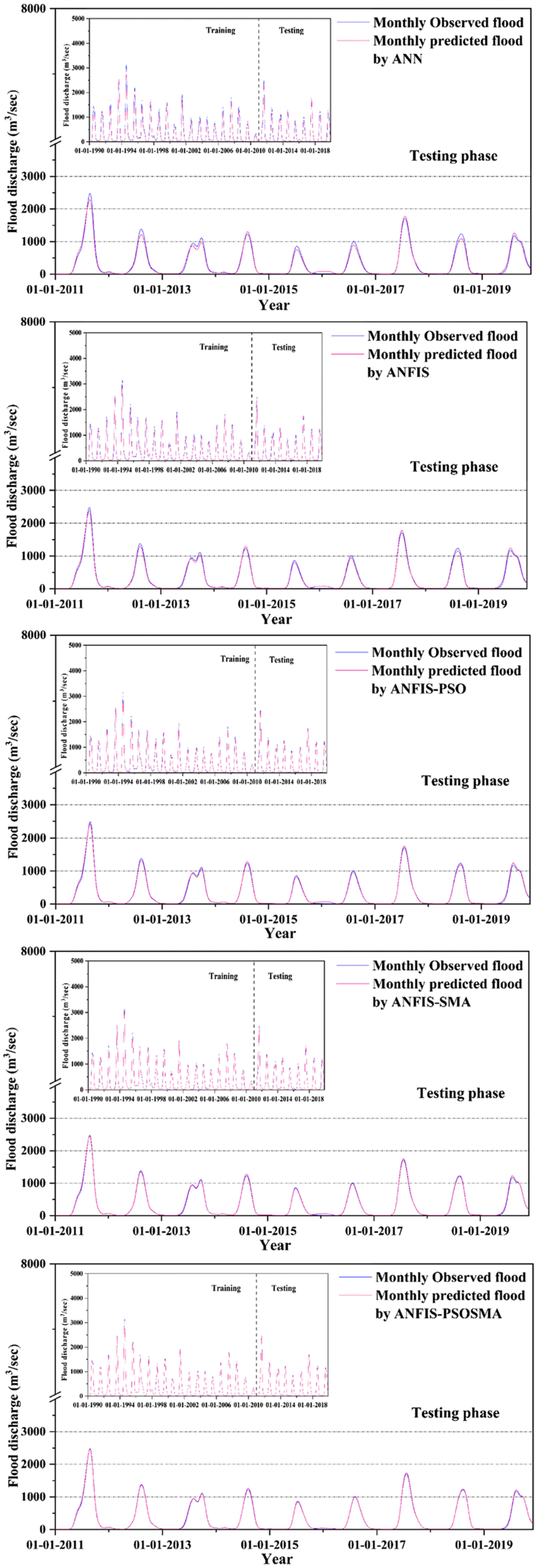

(b)

Fig. 7 (continued)

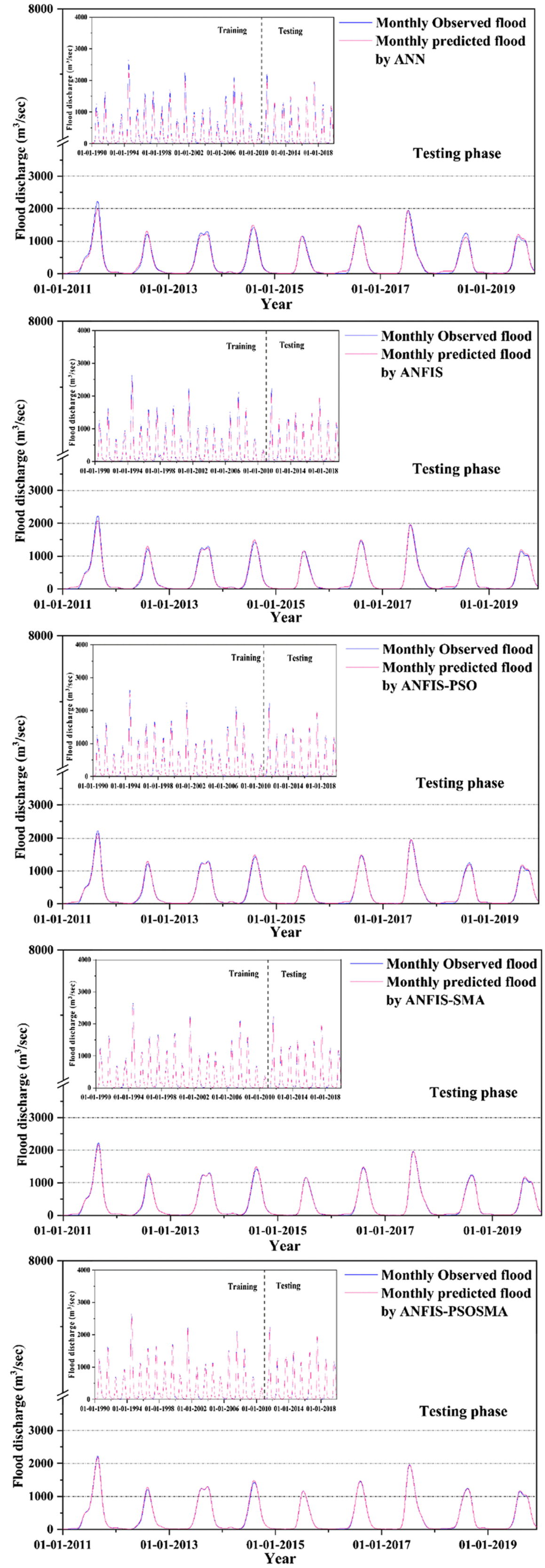

(c)

Fig. 7 (continued)

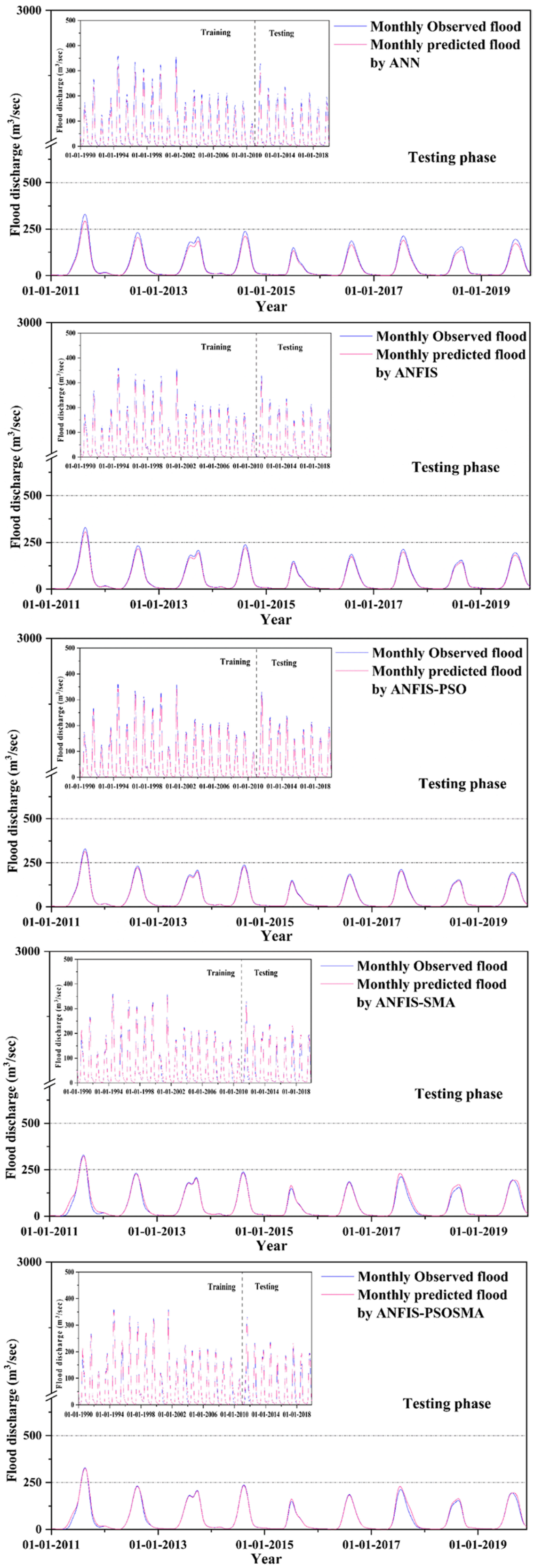

(d)

Fig. 7 (continued)

EEMD or EMD) may be considered for improving models' effectiveness.

Conclusion

This research investigates the possibilities of modelling flood extremes utilising the newly developed AI approaches for improving early flood warning systems to mitigate the effect of flood hazards in the future. The present study was conducted for improving the appropriateness of ANFIS model integrated with PSOSMA for estimating flood discharge. Analysis of outcomes revealed that ANFIS in combination with meta-heuristic algorithms has great potential in estimating Q_{FD} with high accurateness and can enhance performance of standalone ANFIS by evading from the possibility of being stuck in local optima. It also decreases the dependency on conditions of the specified problem and improves search technique and capability of optimising complex problems. A good agreement was achieved amid observed and predicted values for simulated Q_{FD} in Bramhani River.

- Among all employed AI models, ANFIS-PSOSMA model provided superior accurateness compared to other models namely ANFIS-SMA, ANFIS-PSO, ANFIS, and ANN. Novel ANFIS-PSOSMA model gave best value of $R^2 = 0.9946$ than ANFIS-SMA (0.9813), ANFIS-PSO (0.9748), ANFIS (0.9657), and ANN (0.9507) models.
- Addition of evapotranspiration as input to models showed substantial enhancement; hence for building an excellent Q_{FD} prediction model, rainfall data should be taken into consideration. In terms of accuracy in predicting Q_{FD}, it appears that the employed hybrid models performed very well.
- Therefore, the hybrid ANFIS algorithm without the need for an innovative mathematical model is excellent for mimicking the non-linear restraints of obtained data and could be useful as a Q_{FD} estimation tool. To forecast Q_{FD}, identical algorithms with related model architectures could be taken and verified worldwide.
- Provided that usage of better-quality datasets in ANN models will give more consistent results, however, accessibility of these high-quality hydro-climatic data series is one of the major limitations of these types of approaches. For future studies, efforts should be made for applying other appropriate EA and investigating their capability by comparing the models recommended in this work. Also, proposed EA techniques can be applied in other popular AI models that might face certain problems during training phase.

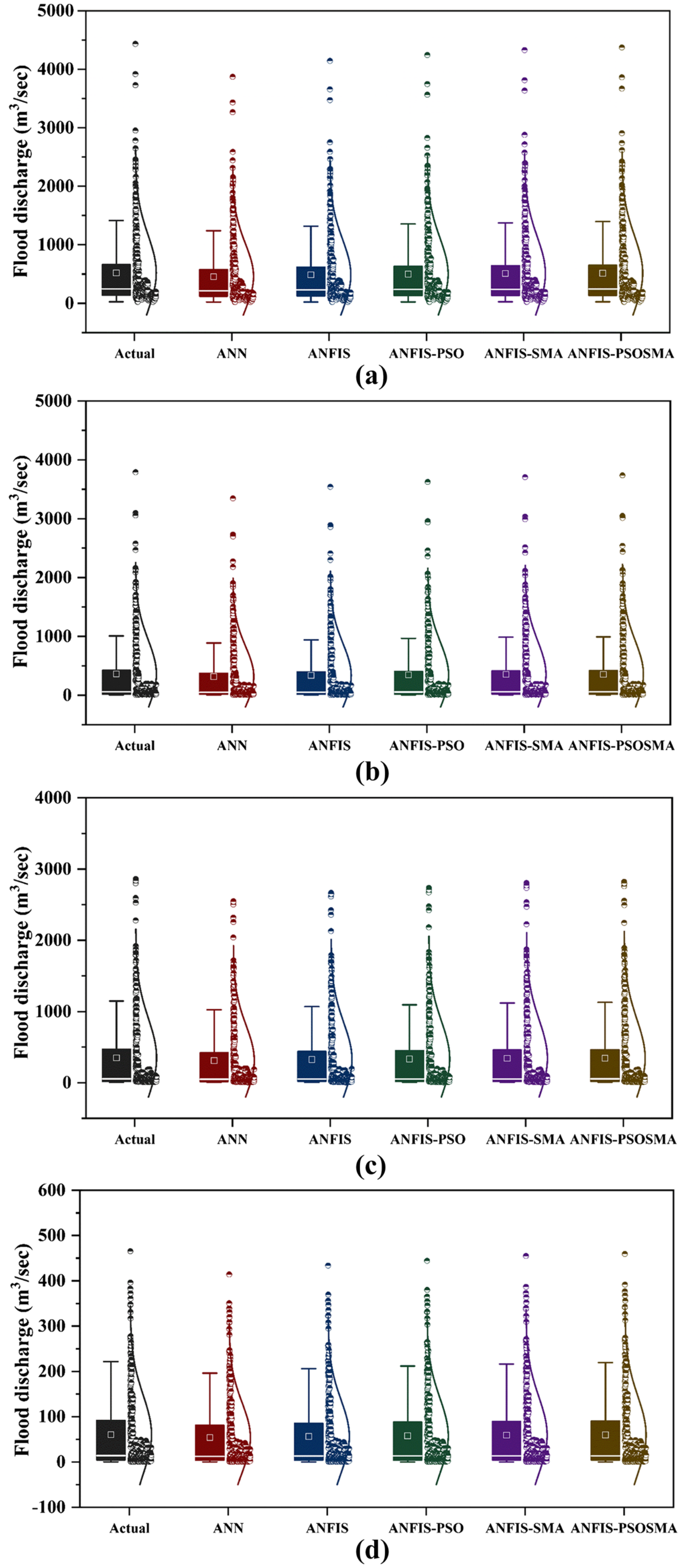

Fig. 8 Boxplot representation for proposed models for **a** Tilga, **b** Jaraikela, **c** Gomlai, and **d** Jenapur stations

Fig. 9 Histogram plots showing frequency of actual and predicted data **a** Tilga, **b** Jaraikela, **c** Gomlai, and **d** Jenapur

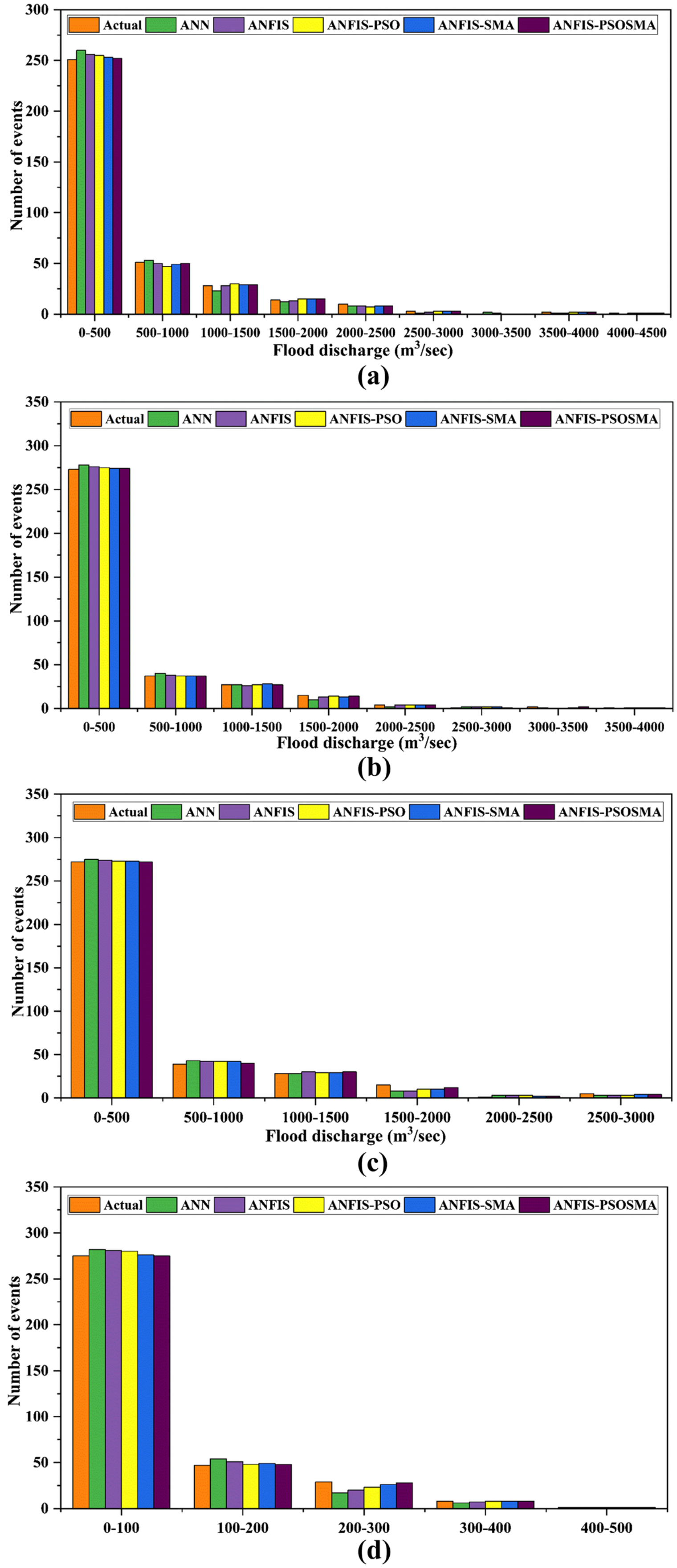

Author contribution Sandeep Samantaray: conceptualisation, analysis, writing-original draft. Abinash Sahoo: formulation, analysis, validation, review, and editing. Pratik Sahoo: methodology, review, and editing. Deba Prakash Satapathy: supervision and validation.

Data availability The data for the current study are available on reasonable request from the corresponding author.

Declarations

Ethics approval and consent to participate Not applicable.

Consent for publication Not applicable.

Competing interests The authors declare no competing interests.

References

Akrami SA, El-Shafie A, Jaafar O (2013) Improving rainfall forecasting efficiency using modified adaptive neuro-fuzzy inference system (MANFIS). Water Resour Manag 27(9):3507–3523

Anusree K, Varghese KO (2016) Streamflow prediction of Karuvannur River Basin using ANFIS, ANN and MNLR models. Procedia Technol 24:101–108. https://doi.org/10.1016/j.protcy.2016.05.015

Arya Azar N, Ghordoyee Milan S, Kayhomayoon Z (2021) Predicting monthly evaporation from dam reservoirs using LS-SVR and ANFIS optimized by Harris hawks optimization algorithm. Environ Monit Assess 193(11):1–14. https://doi.org/10.1007/s10661-021-09495-z

Azad A, Farzin S, Kashi H, Sanikhani H, Karami H, Kisi O (2018) Prediction of river flow using hybrid neuro-fuzzy models. Arab J Geosci 11(22):1–14. https://doi.org/10.1007/s12517-018-4079-0

Breiman L (2001) Random forests. Mach Learn 45(1):5–32

Cai M, Yin Y, Xie M (2009) Prediction of hourly air pollutant concentrations near urban arterials using artificial neural network approach. Transp Res Part D: Transp Environ 14(1):32–41

Chau KW, Wu CL, Li YS (2005) Comparison of several flood forecasting models in Yangtze River". J Hydrol Eng 10(6):485–491. https://doi.org/10.1061/(ASCE)1084-0699(2005)10:6(485)

Chaudhury S, Samantaray S, Sahoo A, Bhagat B, Biswakalyani C, Satapathy DP (2022) "Hybrid ANFIS-PSO Model for Monthly Precipitation Forecasting." In Evolution in Computational Intelligence (pp. 349–359). Springer, Singapore. https://doi.org/10.1007/978-981-16-6616-2_33

Das UK, Samantaray S, Ghose DK, Roy P (2019) Estimation of aquifer potential using BPNN, RBFN, RNN, and ANFIS. In: Smart intelligent computing and applications: proceedings of the Second International Conference on SCI 2018, vol 2. Springer Singapore, pp 569–576

Dawson CW, Abrahart RJ, Shamseldin AY, Wilby RL (2006) Flood estimation at ungauged sites using artificial neural networks. J Hydrol 319(1–4):391–409. https://doi.org/10.1016/j.jhydrol.2005.07.032

Dehghani M, Seifi A, Riahi-Madvar H (2019) Novel forecasting models for immediate-short-term to long-term influent flow prediction by combining ANFIS and grey wolf optimization. J Hydrol 576:698–725. https://doi.org/10.1016/j.jhydrol.2019.06.065

Deo RC, Wen X, Qi F (2016) A wavelet-coupled support vector machine model for forecasting global incident solar radiation using limited meteorological dataset. Appl Energy 168:568–593

Dhunny AZ, Seebocus RH, Allam Z, Chuttur MY, Eltahan M, Mehta H (2020) Flood prediction using artificial neural networks: empirical evidence from Mauritius as a case study. Knowl Eng Data Sci 3(1):1–10

Do Hoai N, Udo K, Mano A (2011) Downscaling global weather forecast outputs using ANN for flood prediction. J Appl Math. https://doi.org/10.1155/2011/246286

Ehteram M, Afan HA, Dianatikhah M, Ahmed AN, Ming Fai C, Hossain MS, Allawi MF, Elshafie A (2019) Assessing the predictability of an improved ANFIS model for monthly streamflow using lagged climate indices as predictors. Water 11(6):1130. https://doi.org/10.3390/w11061130

El-Shafie A, Jaafer O, Akrami SA (2011) Adaptive neuro-fuzzy inference system based model for rainfall forecasting in Klang River, Malaysia. Int J Phys Sci 6(12):2875–2888

Elsafi SH (2014) Artificial neural networks (ANNs) for flood forecasting at Dongola Station in the River Nile, Sudan. Alex Eng J 53(3):655–662. https://doi.org/10.1016/j.aej.2014.06.010

Emami H, Emami S (2021) Application of Whale Optimization Algorithm Combined with Adaptive Neuro-Fuzzy Inference System for Estimating Suspended Sediment Load. J Soft Comput Civ Eng 5(3):1–14. https://doi.org/10.22115/SCCE.2021.281972.1300

Fadaee M, Mahdavi-Meymand A, Zounemat-Kermani M (2022) Suspended sediment prediction using integrative soft computing models: on the analogy between the butterfly optimization and genetic algorithms. Geocarto Int 37(4):961–977. https://doi.org/10.1080/10106049.2020.1753821

Fan C, Sun Y, Zhao Y, Song M, Wang J (2019) Deep learning-based feature engineering methods for improved building energy prediction. Appl Energy 240:35–45

Ghalkhani H, Golian S, Saghafian B, Farokhnia A, Shamseldin A (2013) Application of surrogate artificial intelligent models for real-time flood routing. Water Environ J 27(4):535–548. https://doi.org/10.1111/j.1747-6593.2012.00344.x

Ghose DK, Samantaray S (2019) Estimating runoff using feed-forward neural networks in scarce rainfall region. In: Smart intelligent computing and applications: proceedings of the Second International Conference on SCI 2018, vol 1. Springer Singapore, pp 53–64

Han D, Kwong T, Li S (2007) Uncertainties in real-time flood forecasting with neural networks. Hydrol Process: Int J 21(2):223–228. https://doi.org/10.1002/hyp.6184

Haznedar B, Kilinc HC (2022) A Hybrid ANFIS-GA Approach for Estimation of Hydrological Time Series. Water Resour Manage 36(12):4819–4842. https://doi.org/10.1007/s11269-022-03280-4

Huang Y, Liu Y, Liu Y, Li H, Knievel JC (2019) Mechanisms for a record-breaking rainfall in the coastal metropolitan city of Guangzhou, China: observation analysis and nested very large eddy simulation with the WRF model. J Geophys Res Atmos 124(3):1370–1391

Inyang UG, Akpan EE, Akinyokun OC (2020) A hybrid machine learning approach for flood risk assessment and classification. Int J Comput Intell Appl 19(02):2050012. https://doi.org/10.1007/s11069-016-2220-5

Jamei M, Ali M, Malik A, Prasad R, Abdulla S, Yaseen ZM (2022) Forecasting Daily Flood Water Level Using Hybrid Advanced Machine Learning Based Time-Varying Filtered Empirical Mode Decomposition Approach. Water Resour Manage 36(12):4637–4676. https://doi.org/10.1007/s11269-022-03270-6

Jang JS (1993) ANFIS: adaptive-network-based fuzzy inference system. IEEE Transactions on Systems, Man, and Cybernetics 23(3):665–685

Kennedy J, Eberhart R (1995) Particle swarm optimization. Proceedings of ICNN'95 - International Conference on Neural Networks, vol.4. Perth, WA, Australia, pp. 1942-1948. https://doi.org/10.1109/ICNN.1995.488968

Kim J, Han H, Johnson LE, Lim S, Cifelli R (2019) Hybrid machine learning framework for hydrological assessment. J Hydrol 577:123913

Kisi O, Sanikhani H, Cobaner M (2017) Soil temperature modeling at different depths using neuro-fuzzy, neural network, and genetic programming techniques. Theor Appl Climatol 129:833–848

Kisi O, Shiri J, Karimi S, Adnan RM (2018) Three different adaptive neuro fuzzy computing techniques for forecasting long-period daily streamflows. Big data in engineering applications. pp 303–321

Kheradpisheh Z, Talebi A, Rafati L, Ghaneian MT, Ehrampoush MH (2015) Groundwater quality assessment using artificial neural network: a case study of Bahabad plain, Yazd, Iran. Desert 20(1):65–71

Latt ZZ, Wittenberg H (2014) Improving flood forecasting in a developing country: a comparative study of stepwise multiple linear regression and artificial neural network. Water Resour Manag 28:2109–2128

Li S, Chen H, Wang M, Heidari AA, Mirjalili S (2020) Slime mould algorithm: a new method for stochastic optimization. Futur Gener Comput Syst 111:300–323

Liang J, Li W, Bradford SA, Šimůnek J (2019) Physics-informed data-driven models to predict surface runoff water quantity and quality in agricultural fields. Water 11(2):200

Malik A, Tikhamarine Y, Sihag P, Shahid S, Jamei M, Karbasi M (2022) Predicting daily soil temperature at multiple depths using hybrid machine learning models for a semi-arid region in Punjab, India. Environ Sci Pollut Res 29(47):71270–71289

Mandal S, Saha D, Banerjee T (2005) A neural network based prediction model for flood in a disaster management system with sensor networks. In Proceedings of 2005 International Conference on Intelligent Sensing and Information Processing, 2005. (pp. 78–82). IEEE. https://doi.org/10.1109/ICISIP.2005.1529424

Mekanik F, Imteaz MA, Talei A (2016) Seasonal rainfall forecasting by adaptive network-based fuzzy inference system (ANFIS) using large scale climate signals. Clim Dyn 46:3097–3111

McCulloch WS, Pitts W (1943) A logical calculus of the ideas immanent in nervous activity. The Bulletin of Mathematical Biophysics 5:115–133

Mirboluki A, Mehraein M, Kisi O (2022) Improving accuracy of neuro fuzzy and support vector regression for drought modelling using grey wolf optimization. Hydrol Sci J 67(10):1582–1597. https://doi.org/10.1080/02626667.2022.2082877

Mitra P, Ray R, Chatterjee R, Basu R, Saha P, Raha S, Barman R, Patra S, Biswas SS, Saha S (2016) Flood forecasting using Internet of things and artificial neural networks. In 2016 IEEE 7th Annual Information Technology, Electronics and Mobile Communication Conference (IEMCON) (pp. 1–5). IEEE. https://doi.org/10.1109/IEMCON.2016.7746363

Mohammadi B, Moazenzadeh R, Christian K, Duan Z (2021) Improving streamflow simulation by combining hydrological process-driven and artificial intelligence-based models. Environ Sci Pollut Res 28(46):65752–65768. https://doi.org/10.1007/s11356-021-15563-1

Mosavi A, Ozturk P, Chau KW (2018) Flood prediction using machine learning models: literature review. Water 10(11):1536

Mukerji A, Chatterjee C, Raghuwanshi NS (2009) Flood forecasting using ANN, neuro-fuzzy, and neuro-GA models. J Hydrol Eng 14(6):647–652

Nayak PC, Sudheer KP, Rangan DM, Ramasastri KS, (2005) Short-term flood forecasting with a neurofuzzy model. Water Resour Res 41(4). https://doi.org/10.1029/2004WR003562

Nguyen PK-T, Chua LH-C (2012) The data-driven approach as an operational real-time flood forecasting model. Hydrol Process 26(19):2878–2893. https://doi.org/10.1002/hyp.8347

Othman F, Naseri M (2011) Reservoir inflow forecasting using artificial neural network. Int J Phys Sci 6(3):434–440

Panahi F, Ehteram M, Emami M (2021) Suspended sediment load prediction based on soft computing models and Black Widow Optimization Algorithm using an enhanced gamma test. Environ Sci Pollut Res 28(35):48253–48273. https://doi.org/10.1007/s11356-021-14065-4

Patel N, Bhoi AK, Paika DK, Sahoo A, Mohanta NR, Samantaray S (2022) Water Table Depth Forecasting Based on Hybrid Wavelet Neural Network Model. In Evolution in Computational Intelligence (pp. 233–242). Springer, Singapore. https://doi.org/10.1007/978-981-16-6616-2_22

Penghui L, Ewees AA, Beyaztas BH, Qi C, Salih SQ, Al-Ansari N, Bhagat SK, Yaseen ZM, Singh VP (2020) Metaheuristic optimization algorithms hybridized with artificial intelligence model for soil temperature prediction: Novel model. IEEE Access 8:51884–51904. https://doi.org/10.1109/ACCESS.2020.2979822

Peyghami MR, Khanduzi R (2013) Novel MLP neural network with hybrid tabu search algorithm. Neural Network World 23(3):255

Sahoo A, Samantaray S, Ghose DK (2022a) Multilayer perceptron and support vector machine trained with grey wolf optimiser for predicting floods in Barak river, India. J Earth Syst Sci 131(2):1–23. https://doi.org/10.1007/s12040-022-01815-2

Sahoo A, Mohanta NR, Samantaray S, Satapathy DP (2022b) Application of Hybrid ANFIS-CSA Model in Suspended Sediment Load Prediction. In Advanced Computing and Intelligent Technologies (pp. 295–305). Springer, Singapore. https://doi.org/10.1007/978-981-19-2980-9_24

Samani S, Vadiati M, Nejatijahromi Z, Etebari B, Kisi O (2022) Groundwater level response identification by hybrid wavelet–machine learning conjunction models using meteorological data. Environ Sci Pollut Res 1–22. https://doi.org/10.1007/s11356-022-23686-2

Samantaray S, Ghose DK (2019) Dynamic modelling of runoff in a watershed using artificial neural network. In: Smart intelligent computing and applications: proceedings of the Second International Conference on SCI 2018, vol 2. Springer, Singapore, pp 561–568

Samantaray S, Ghose DK (2022) Prediction of S12-MKII rainfall simulator experimental runoff data sets using hybrid PSR-SVM-FFA approaches. Journal of Water and Climate Change 13(2):707–734

Samantaray S, Sahoo A, Satapathy DP, Mishra SS (2022a) Prophecy of groundwater fluctuation through SVM-FFA hybrid approaches in arid watershed, India. In Current Directions in Water Scarcity Research, Elsevier, pp 341–365 https://doi.org/10.1016/B978-0-323-91910-4.00020-0

Samantaray S, Sahoo A, Sathpathy DP (2022b) Temperature Prediction Using Hybrid MLP-GOA Algorithm in Keonjhar, Odisha: A Case Study. In Smart Intelligent Computing and Applications, (pp. 319–330). Singapore: Springer Nature Singapore. https://doi.org/10.1007/978-981-16-9669-5_29

Samantaray S, Sahoo A, Mishra SS (2022c) Flood forecasting using novel ANFIS-WOA approach in Mahanadi river basin, India. In Current Directions in Water Scarcity Research. Elsevier, pp 663–682. https://doi.org/10.1016/B978-0-323-91910-4.00037-6

Samantaray S, Sahoo A, Satapathy DP (2022d) Prediction of groundwater-level using novel SVM-ALO, SVM-FOA, and SVM-FFA algorithms at Purba-Medinipur, India. Arab J Geosci 15(8):1–22. https://doi.org/10.1007/s12517-022-09900-y

Samantaray S, Sah MK, Chalan MM, Sahoo A, Mohanta NR (2022e) Runoff Prediction Using Hybrid SVM-PSO Approach. In Data Engineering and Intelligent Computing (pp. 281–290). Springer, Singapore. https://doi.org/10.1007/978-981-19-1559-8_29

Samantaray S, Sahoo A, Paul S, Ghose DK (2022f) Prediction of Bed-Load Sediment Using Newly Developed Support-Vector Machine Techniques. J Irrig Drain Eng 148(10):04022034. https://doi.org/10.1061/(ASCE)IR.1943-4774.0001689

Samantaray S, Biswakalyani C, Singh DK, Sahoo A, Prakash Satapathy D (2022g) Prediction of groundwater fluctuation based on hybrid

ANFIS-GWO approach in arid Watershed, India. Soft Computing 26(11):5251–5273. https://doi.org/10.1007/s00500-022-07097-6
Sarkar BN, Samantaray S, Kumar U, Ghose DK (2021) Runoff is a key constraint toward water table fluctuation using neural networks: a case study. Communication software and networks: proceedings of INDIA 2019. Springer Singapore, pp 737–745
Seifi A, Ehteram M, Singh VP, Mosavi A (2020) Modeling and uncertainty analysis of groundwater level using six evolutionary optimization algorithms hybridized with ANFIS, SVM, and ANN. Sustainability 12(10):4023
Singh RM (2012) Wavelet-ANN model for flood events. In Proceedings of the International Conference on Soft Computing for Problem Solving (SocProS 2011) (pp. 165–175). Springer, New Delhi. https://doi.org/10.1007/978-81-322-0491-6_16
Singh UK, Kumar B, Gantayet NK, Sahoo A, Samantaray S,Mohanta, NR (2022) A Hybrid SVM–ABC Model for Monthly Stream Flow Forecasting. In Advances in Micro-Electronics, Embedded Systems and IoT (pp. 315–324). Springer, Singapore. https://doi.org/10.1007/978-981-16-8550-7_30
Sridharam S, Sahoo A, Samantaray S, Ghose DK (2021) Assessment of flow discharge in a river basin through CFBPNN, LRNN and CANFIS. In Communication software and networks (pp. 765–773). Springer, Singapore. https://doi.org/10.1007/978-981-15-5397-4_78
Tabbussum R, Dar AQ (2021) Performance evaluation of artificial intelligence paradigms—artificial neural networks, fuzzy logic, and adaptive neuro-fuzzy inference system for flood prediction. Environ Sci Pollut Res 28(20):25265–25282
Tao H, Diop L, Bodian A, Djaman K, Ndiaye PM, Yaseen ZM (2018) Reference evapotranspiration prediction using hybridized fuzzy model with firefly algorithm: Regional case study in Burkina Faso. Agric Water Manag 208:140–151. https://doi.org/10.1016/j.agwat.2018.06.018
Tsakiri K, Marsellos A, Kapetanakis S (2018) Artificial neural network and multiple linear regression for flood prediction in Mohawk River, New York. Water 10(9):1158. https://doi.org/10.3390/w10091158
Ullah N, Choudhury P (2010) Flood forecasting in river system using ANFIS. In AIP Conference Proceedings. Am Inst Phys 1298(1):694–699 https://doi.org/10.1063/1.3516407
Vapnik V (1995) The nature of statistical learning theory. Springer, New York, NY, USA
Wang J, Cui Q, He M (2022) Hybrid intelligent framework for carbon price prediction using improved variational mode decomposition and optimal extreme learning machine. Chaos Solitons Fractals. 156:111783. https://doi.org/10.1016/j.chaos.2021.111783
Wu CL, Chau KW (2006) A flood forecasting neural network model with genetic algorithm. Int J Environ Pollut 28(3–4):261–273
Xiao K, Li G, Li H, Zhang Y, Wang X, Hu W, Zhang C (2019) Combining hydrological investigations and radium isotopes to understand the environmental effect of groundwater discharge to a typical urbanized estuary in China. Sci Total Environ 695:133872
Yaseen ZM, Ghareb MI, Ebtehaj I, Bonakdari H, Siddique R, Heddam S, Yusif DR (2018) Rainfall pattern forecasting using novel hybrid intelligent model based ANFIS-FFA. Water Resour Manage 32(1):105–122. https://doi.org/10.1007/s11269-017-1797-0
Yaseen ZM, Mohtar WHMW, Ameen AMS, Ebtehaj I, Razali SFM, Bonakdari H, Salih SQ, Al-Ansari N, Shahid S (2019) Implementation of univariate paradigm for streamflow simulation using hybrid data-driven model: Case study in tropical region. IEEE Access 7:74471–74481. https://doi.org/10.1109/ACCESS.2019.2920916
Zia H, Harris N, Merrett G, Rivers M (2015) Predicting discharge using a low complexity machine learning model. Comput Electron Agric 118:350–360
Zhou SL, McMahon TA, Walton A, Lewis J (2002) Forecasting operational demand for an urban water supply zone. J Hydrol 259:189–202

Publisher's note Springer Nature remains neutral with regard to jurisdictional claims in published maps and institutional affiliations.